Planet-Detection Simulations for Several Possible TESS Extended Missions

Luke Bouma, Josh Winn, Jacobi Kosiarek, Peter McCullough

October 12, 2016

Executive Summary

The Transiting Exoplanet Survey Satellite (*TESS*) will perform a two-year, nearly all-sky survey for transiting exoplanets. There do not appear to be any fundamental obstacles to continuing science operations for at least several years after this Primary Mission. Any Extended Mission will likely need to be organized while the Primary Mission is occupying most of the TESS team's full attention. The purpose of this Memo, and the accompanying Wiki document, is to provide a head start to those who are planning and proposing for an Extended Mission.

The choice of an Extended Mission is likely to be influenced by many factors besides the prospects for planet detection. We have created an editable document on the TESS wiki to raise and discuss those broad issues. This Memo is narrowly focused on planet detection. We try to anticipate the quantities and types of planets that would be detected during several plausible scenarios for a one-year Extended Mission following the two-year Primary Mission. We use Monte Carlo simulations to compare different strategies for scanning the sky during one year of operations, and try to interpret the results and their implications for future years. For simplicity we do not compare different choices for the cadence of photometric measurements or in the metrics for target selection, although different choices might prove to be advantageous and should be studied in future work.

Throughout this report we consider six different scenarios for Year 3 of the TESS mission, illustrated in Figure 2:

1. *HEMI*, which re-observes one of the ecliptic hemispheres in essentially the same manner as in the Primary Mission (i.e., neglecting the zone within 6° of the ecliptic);
2. *HEMI+ECL*, which re-observes one of the ecliptic hemispheres, but this time covering the entire hemisphere at the expense of the continuous-viewing zone near the pole;
3. *POLE*, which focuses on one of the two ecliptic poles;
4. *ECL-LONG*, which has a series of pointings with the long axis of the field-of-view along the ecliptic (in combination with some fields near the ecliptic pole, when the Earth or Moon would prevent effective observations of the ecliptic);
5. *ECL-SHORT*, which has a series of pointings with the short axis of the field-of-view along the ecliptic (again in combination with some fields near the ecliptic pole);
6. *ALLSKY*, which covers nearly the entire sky with 14-day pointings (as opposed to the 28-day pointings of the Primary Mission), by alternating between northern and southern hemispheres.

We simulate the results based on the methodology of Sullivan et al. [2015], after bug fixes and enhancements by Luke Bouma in consultation with Josh Winn. Additional inputs were provided by Jacobi Kosiarek and Peter McCullough, as described in the text.

Some of the most important findings are:

1. The overall quantity of detected planets does not depend strongly on the sky-scanning schedule. Among the six scenarios considered here, the number of newly-detected sub-Neptune planets is the same to within about 30%.
2. The number of newly-detected sub-Neptune planets in Year 3 is approximately the same as the number detected in either Year 1 or Year 2. Thus, we do not expect a sharp fall-off in the planet discovery rate in Year 3. This is because the Primary Mission will leave behind many short-period transiting planets with bright host stars, with a signal-to-noise ratio just below the threshold for detection. These planets can be detected by collecting more data in Year 3.
3. Regarding newly detected sub-Neptunes, the `ALLSKY`, `POLE`, and `HEMI+ECL` strategies offer the greatest number (1300-1400, as compared to the 1250 during each year of the Primary Mission).
4. Regarding planets with orbital periods $\gtrsim 20$ days, the `ALLSKY`, `POLE`, and `HEMI` strategies would discover twice as many such planets as will be discovered in each year of the Primary Mission. This would help to overcome one of the main limitations of the Primary Mission: the strong bias toward shorter orbital periods.
5. Regarding new planets with very bright host stars ($I_c < 10$), the `ALLSKY`, `HEMI+ECL`, and `ECL-SHORT` strategies offer the greatest num-

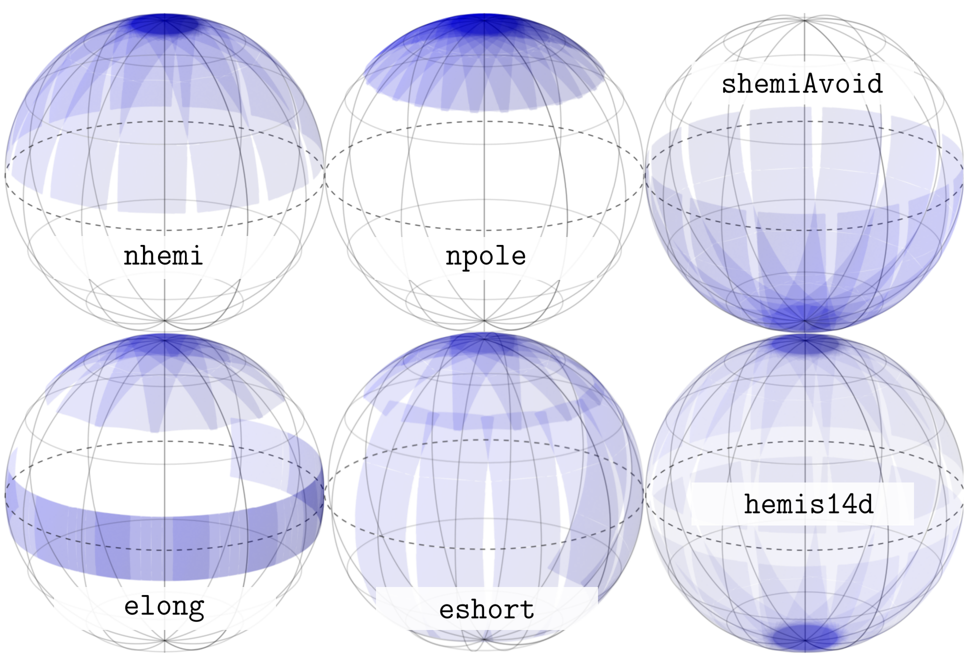

Figure 1: Six proposed pointing strategies for a *TESS* extended mission, visualized in ecliptic coordinates. Note that none of these scenarios spend the entire year observing the ecliptic; we concluded that such a plan would be inadvisable because of interruptions by the Earth and Moon (see Fig. 10).

bers (∼190, about the same as are found in each year of the Primary Mission; see Table 2).

6. Regarding planets with near-terrestrial insolation ($0.2 < S/S_\odot < 2$), all the strategies considered here offer similar numbers (about 120, as compared to 105 in each year of the Primary Mission).

7. Apart from detecting new planets, a potentially important function of an Extended Mission would be to improve our ability to predict the times of future transits and eclipses of TESS-detected planets. With data from the Primary Mission alone, the uncertainty in transit ephemerides will inhibit follow-up observations after only a few years.

The rest of this report is organized as follows. Sec. 3 discusses how we selected and compared different pointing strategies, as well as how we modeled *TESS*'s observations and planet detections. Sec. 3.7 gives a list of the most important assumptions we made for the simulations. Sec. 4 compares the simulated populations of newly-detected planets, for the 6 different scenarios under consideration. Sec. 5.1) discusses some considerations and implications for future years of the Extended Mission, beyond the one-year scenarios that were simulated in detail. Sec. 5.2) discusses the critical issue of the uncertainty in transit ephemerides. Sec. 5.3 discusses the reliability and limitations of our methodology. Sec. 6 presents our conclusions, and recommends avenues for further study.

Contents

1 *Executive Summary*

TESS is scheduled to launch in December of 2017. The primary mission will run for two years, and the *TESS* Science Office will submit a proposal for an extended mission to NASA's senior review of operating missions in early 2020. In this report we lay out technical requirements, science goals, opportunities, and risks that will impact the decision of how *TESS* should observe after completing its primary mission.

Building on Sullivan et al. [2015], we perform Monte Carlo simulations of the population of planets that *TESS* will detect for the Year-3 observing strategies shown in Fig. 2. None of our proposed strategies entail observing the ecliptic for an entire year. For ~ 4 months of such a scenario, the Earth and Moon cross *TESS*'s field of view at a drastically higher rate than during the rest of the year (Fig. 10). We circumvent this issue by proposing `ECL-LONG` and `ECL-SHORT`. We also note in passing that `ALLSKY` spends a single spacecraft orbit ($\sim$14 days) per field, 'zig-zagging' across the sky.

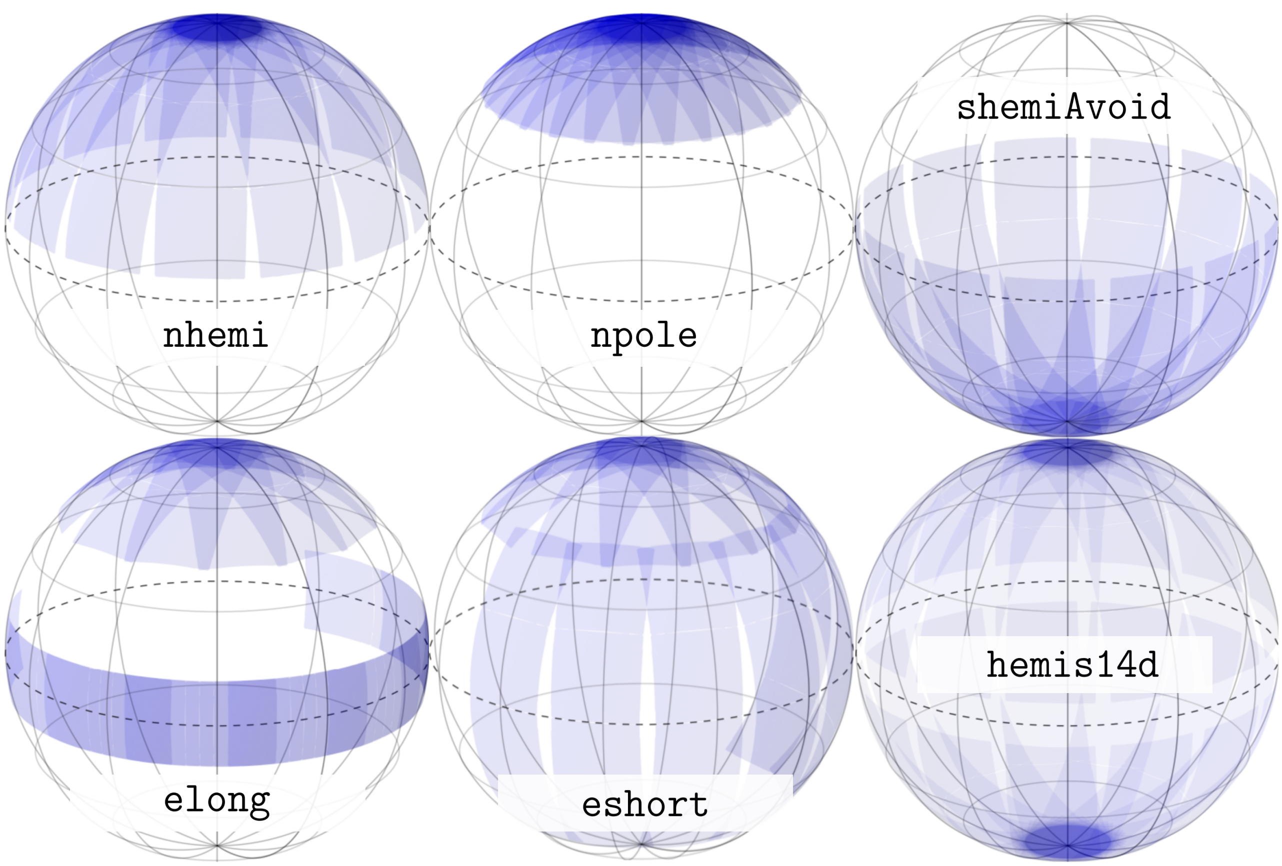

Figure 2: Six proposed pointing strategies for a *TESS* extended mission, visualized in ecliptic coordinates. Earth and moon crossings make looking at the ecliptic for an entire year impractical (see Fig. 10).

The most notable result from these simulations is that a third year's extended mission will yield as many new sub-Neptune radius planets as either Years 1 or 2 – roughly 1250. The means that extended missions will be valuable because they will detect a large number of small planets. This holds regardless of where on the sky observe, with the newly detected planet yields varying by $\lesssim 30\%$ between our six proposed scenarios.

Another notable result is that it will be possible to detect about as many new $P > 20$ day planets in one year of *TESS*'s extended mission are in both years of the primary mission. This result derives both from turning high-SNR single-transit events from the primary into double and triple-transit events (giving more transits over which to phase-fold and lower the in-transit noise), as well as by turning low-SNR multiple-transit events into threshold-crossing[1] events.

[1] Following Sullivan et al. [2015], we rule a planet detected if SNR > 7.3 and $N_{\rm tra} \geq 2$.

An additional result, relevant to both the primary and extended missions, is that our simulations approximate the effect of the Earth and Moon crossing through *TESS*'s field of view (Sec. 3.6). Running the primary mission without accounting for Earth and Moon losses returns a mean of 2678 detected planets with $R_p < 4R_\oplus$, while running them with Earth and Moon crossings gives 2482 such planets on average. This is a loss of 196 planets, or 7% of the sub-Neptune yield.

Assessing pointing strategies based on yield statistics Different extended mission pointings perform better and worse by different metrics. We focus only on detected planets with $R_p < 4R_\oplus$ (Fig. 15). In terms of absolute sub-Neptune radius planet yield, `ALLSKY`, `POLE`, and `HEMI+ECL` offer the most new planets (1300-1400, compared to the primary mission's 2500). `ALLSKY`, `POLE`, and `HEMI` offer the most new long period planets (250-300, compared to the primary mission's 290). `ALLSKY`, `HEMI+ECL`, and `ECL-SHORT` offer the most new planets orbiting $I_c < 10$ hosts ($\sim$190, compared to the primary's 385; see Table 2). They all offer similar numbers of new habitable zone planets (about 120, to the primary's 210)[2]. `POLE` is the worst at detecting new planets with atmospheres that are amenable for atmospheric follow-up, but extended missions only yield $10 - 25$ such planets, compared to the primary mission's $\sim$110.[3]

[2] We let 'habitable zone' mean that the planet insolation S is within $0.2S_\oplus - 2S_\oplus$. The physically-motivated Kopparapu et al. [2013] HZ gives roughly a third of our quoted numbers (Fig. 20).

[3] We let 'amenable for atmospheric follow-up' mean $\mathrm{SNR}_{\rm atm} > \mathrm{SNR}_{\rm GJ\ 1214b}/4$, where $\mathrm{SNR}_{\rm atm}$ refers to the signal-to-noise of the planet in transmission over 4 transits observed by *JWST*'s NIRISS instrument, and the normalization is $\mathrm{SNR}_{\rm atm}$ for GJ 1214b. Dividing by a factor of four helps avoid small-number fluctuations. Note for *JWST* follow-up the ecliptic latitude of the detections also matters (see following footnote).

An important assumption behind these statistics is that we assume 2 transits and a phase-folded SNR of 7.3 are sufficient for detection. `ALLSKY` is more dependent on this assumption than any other scenario: it detects the most new planets and the most new $P > 20$ day planets, but if we were to modify our detection requirement to $N_{\rm tra} \geq 3$, roughly half of the long period planets that `ALLSKY` detects would be lost (Fig. 17). Given the overwhelming amount of false alarms that will be present in a transit-search pipeline from $N_{\rm tra} = 2$

events, this is a serious caution against the `ALLSKY` approach. By way of comparison, `POLE` detects most of its long-period planets with ≥ 4 transits.

Desires in exoplanet science: Planet yield statistics are useful, but they are blind to other important considerations. For an extensive discussion of the broad science that can be accomplished with extra *TESS* observations, see LINK!; for a discussion of which opportunities we think affect extended mission planning, see LINK!. Summarizing,

1.) Ephemeris times: The *TESS* mission must provide accurate predictions for when its objects transit to enable successful follow-up efforts.

Following a derivation shown in Sec. 5.2, the uncertainty on the mid-transit times for *TESS* objects of interest, σ_{t_c}, propagates to be roughly

$$\sigma_{t_c}\ [\mathrm{hr}] \approx 2 \times (\text{number of years after detection})\,.$$

This problem is reduced by an order of magnitude if we capture just one transit with a year's baseline after the initial detection (Figs. 24, 25). This argues strongly for an extended mission which, whether over 1 or 2 years, re-observes many of the targets that *TESS* detects in its primary mission. The smallest-radius Earths and super-Earths may otherwise be difficult to recover.

2.) Follow-up of TESS objects

2.1) JWST: TESS should detect the most promising planets for *JWST* follow-up[4] after only a year's observation (see table & discussion at LINK!). This means that *TESS* is not 'bound' to the ecliptic poles in an extended mission to support *JWST*'s target selection. More important for ensuring *JWST*–*TESS* overlap will be the efficient spectroscopic and photometric follow-up of *TESS*'s planets from the ground; by *JWST*'s launch in October 2018, only a few verified *TESS* planets will be known.

[4] We let 'promising planets for *JWST* follow-up' mean those that have $R_p < 4R_\oplus$, $\mathrm{SNR}_{\mathrm{atm}} > \mathrm{SNR}_{\mathrm{GJ\ 1214b}}/5$, and absolute ecliptic latitude $|\beta| > 80°$ so that they can be observed for more than two-thirds of the year by *JWST*.

2.2) CHEOPSs' visibility is best near the ecliptic, and non-existent near the ecliptic poles. Extended missions that focus exclusively on the ecliptic poles neglect *TESS* and *CHEOPS*s' complementarity [Berta-Thompson et al., 2016]. Those that focus on the ecliptic, including `ECL-LONG` and `ECL-SHORT`, provide the largest amount of overlapping coverage, with `HEMI` providing a middle-ground.

2.3) The primary mission will clarify whether the availability of *ground-based follow-up resources* will need to constrain *TESS*'s extended observing. Ideally, it will not.

3.) TESS as a follow-up mission: TESS's target list in the primary mission will include known planet-hosts from transit and RV surveys. Summarizing those that are most strategically important for an extended mission:

3.1) The Kepler field. *TESS* observes the *Kepler* field for $\sim$52 days in 2019 (Fig. 5). An extended mission like `POLE` could observe the field for 104 days per year – twice as long as repeating `HEMI`. The main reasons to allocate extra importance to *Kepler*'s field include: *(a)* measuring transit timing variations over a long baseline; *(b)* confirming few-transit KOI candidates, *(c)* calibrating *TESS* against well-studied candidates, *(d)* continuing observations of circumbinary planets. Sullivan [2013] studied *TESS*'s performance on the field in detail. Scaling his absolute results by a factor of 1.5 (about twice as many KOIs are now known, but they are systematically fainter), we can expect *TESS* to detect $\sim$45 $R_p < 4R_\oplus$ KOIs at $\geq 3\sigma$ per transit.

3.2) K2's fields will have covered $\gtrsim$60% of the area in the $|\beta| < 6°$ band about the ecliptic by the beginning of *TESS*'s extended mission *TESS*'s primary mission does not observe in the $|\beta| < 6°$ band. Our simulated planet populations for both `ECL-LONG` and `ECL-SHORT` assumed no knowledge from *K2* . This is unrealistic. A large fraction of the planets that *TESS* will be capable of detecting near the ecliptic will already either exist as candidates in *K2*'s data or have been discovered[5]. Summarizing then what we find to be the most compelling reasons to observe the ecliptic in an extended *TESS* mission: *(a)* combine *TESS* and *K2* data, doubling the *K2* observing baseline for most targets. In turn, confirm low-SNR candidates, and detect extra transits for a relatively large number of $20 < P < 40$ day planets; *(b)* catch 'holes' in the $|\beta| < 12°$ band that *K2* missed, completing the all-sky search for small planets transiting the brightest stars; *(c)* observe targets in *K2* fields that simply were not selected in *K2*'s $\sim 2 \times 10^4$ per campaign. For instance, *TESS*'s bandpass allows probing down to cooler M dwarfs; *(d)* measure TTVs for targets over baselines up to 5-years. *(e)* confirm a small but significant number of $P > 40$ day planets.

[5] Our coarse estimate is that $\sim$175 of *TESS*'s 500 new $|\beta < 12°|$, $R_p < 4R_\oplus$ detections from `ECL-LONG` would already be detected by *K2* (see Sec. **??**)

Given the central role that combining *TESS* and *K2* data would play if *TESS* were to observe the ecliptic, and given our non-treatment of this question in our yield simulations, we recommend that a detailed study of *K2* and *TESS*'s combined potential be carried out before ruling for or against `ECL-LONG` or `ECL-SHORT`.

3.3) TESS following up ground-based surveys: The north and south skies have similar numbers of known ground-detected transiting and RV planets, so the desire to follow up ground-based surveys probably will not impact *TESS*'s extended mission on a 1-year timescale. Over 2-year timescales, if an extended mission were to focus on a single hemisphere it would neglect half of the known transiting/RV planets, no longer *(a)* discovering additional small transiting companions or *(b)* improving uncertainties in the physical and orbital parameters of known planets.

Desires outside of exoplanet science: We motivate cases for using *TESS* data in asteroseismology, variable-star astronomy (pulsating stars, eruptive stars, supernovae), and solar system astronomy (main belt asteroids) at LINK!. To our understanding an extended mission can observe anywhere on the sky without neglecting these sub-fields. Observational cadence is a more important free-parameter – asteroseismology in particular benefits greatly from short cadence data.

Results summary:

1 year extension: None of the pointing options that we propose are obviously bad (Fig. 15). `ALLSKY` does well under idealized assumptions, but is risky because of aliasing and low N_{tra} issues. However it could be the fastest way to deal with the ephemeris issue. The biggest qualitative difference between looking at and away from the ecliptic is *K2*. *K2* does mean fewer 'new *TESS* planets', but combining the two datasets might lead to many long period planet detections (see recommendations – we did not deal with this quantitatively).

2 year extension: Knowing when *TESS* planets transit is incredibly important for follow-up efforts, and needs to be addressed either through `ALLSKY` or by going 'all-sky' over two years. Although we did not study 2-year extensions in depth, performing the opposite-hemisphere complements of `HEMI`, `POLE`, and `HEMI+ECL` would yield the same large number of new planets as from Year 3. Another reason to observe both hemispheres is to be sure that we have really detected all of the best super-Earths for transmission spectroscopy (Table **??**).

The main reason to repeat one-hemisphere observations indefinitely is to detect long period planets. Our opinion is that the reasons to observe all-sky are more compelling.

Recommendations (expanded in Sec. 6.1):

Analyze target prioritization problem: planet occurrence rates are functionally dependent on a star's properties – should this affect which stars we give upgraded cadence? Is our proposed `Merit` statistic (Eq. 2) how we want to prioritize target stars for short-cadence observations?

Optimize cadence: it may be better for transit detection to observe 4×10^5 target stars at 4 minute cadence, rather than 2×10^5 at 2 minute cadence.

Take steps to address the 'upgrading cadence' problem: if there is a likely transiting planet in full frame image data, upgrading the planet to short cadence in future observing sectors improves the probability and quality of detection.

Guest Investigator Office / TESS Science Office: solicit advice from experts in asteroseismology and variable-sky astronomy to understand how extended missions affect their science cases (*e.g.*, data throughput rates are particularly important for time-sensitive supernovae observations). More broadly, solicit community feedback during the process of defining the extended mission. This may entail a call for white papers, comments on this report, or direct proposals to the GI office.

Decide (explicitly or implicitly) on weights between our proposed metrics. Sec. 3.3 gives a list of considerations that will matter in deciding *TESS*'s extended mission: should we prioritize new planet detection statistics? Broader astronomy, as *K2* did? Are the $\lesssim 30\%$ variations in absolute new planet yields more valuable than other desires or opportunities?

Simulate combining TESS and K2 data for `ECL-LONG` *and* `ECL-SHORT`. This is perhaps the most important qualitative difference between observing towards and away from the ecliptic.

2 *Statement of problem*

Once *TESS*'s primary survey is complete, what should the spacecraft do next? Different observing strategies may benefit different science goals. As a preliminary example, observing a given region of sky for as long as possible allows *TESS* to detect planets with the longest possible orbital periods. However, if we want to discover new small planets around the brightest possible stars, it could be better to target new sky, perhaps near the ecliptic.

This memo is a trade study of a non-exhaustive set of plausible extended mission scenarios. Our main aim is to quantify how different spacecraft-pointings will affect *TESS*'s planet yield. We also briefly discuss the opportunities and risks each observing strategy may present, and give a more detailed discussion at LINK!.

Some important free parameters that will define *TESS*'s extended mission include:

- Where to point the cameras on the sky.
- The duration of proposed observations.
- With a fixed data mass, the relative allocations between short (2 minute) and long (30 minute) cadence images[6].
- The cadence of full frame images; for instance keeping full-frames at 15 minute cadence at the cost of observing fewer short-cadence targets.
- The cadence of postage stamps; for instance stacking them at 4 minute cadence instead of 2 minute cadence, and observing twice as many target stars.
- The target allocation strategy. This includes how to prioritize target stars from the *TESS* Input Catalog. It also involves the question of how to use knowledge obtained from full frame images in the primary mission when re-observing the same fields in an extended mission.

[6] Respectively referred to as 'postage stamps' because the aperture centered on any given star resembles a small-area postage-stamp, and as 'full frame images' since they are the entire CCD readout. The 'postage stamp' target stars are a subset, nominally 2×10^5 stars, of the *TESS* Input Catalog.

In this report, we evaluate how well a set of extended mission spacecraft pointings (for 1 year of extra observing) satisfies different technical requirements and science goals. We also discuss unique opportunities that may be available through each option. The other parameters outlined above, notably the relative allocations between different data products at a fixed data mass, will also impact the primary and extended missions. We recommend that they be studied separately.

2.1 *Outline of report*

We begin in Sec. 3 by discussing how we select and compare different pointing strategies, as well as how we model *TESS*'s observations and planet detections. This includes a summarized list of our assumptions in Sec. 3.7. We then compare the newly detected planet populations from some plausible one-year extended missions in Sec. 4. Newly detected planets are not the only valuable outcome of an extended mission. What that in mind, extrapolating from our single-year simulation, we discuss what may best on a > 1 year horizon for planet detections (Sec. 5.1). This long-term future hinges crucially upon how the uncertainty on the mid-transit times for *TESS* planets scales with time (Sec. 5.2). Discussion of the broader science that *TESS* could and perhaps should perform, as well as opportunities for ground and space-based follow-up, are available at LINK!. We conclude by evaluating the reliability of our methods (Sec. 5.3), and in Sec. 6 present recommendations for what comes next in defining *TESS*'s extended mission.

3 *Approach*

3.1 *Constraints on possible pointing strategies*

The spacecraft has finite fuel reserves for necessary maneuvers, but the reserves are expected to last about 10 years [R. Vanderspek, priv. comm.], well past the three-year time horizon that is the focus of this study.

When considering possible schedules for telescope pointings, the main constraint is that the cameras must be directed approximately opposite the Sun. Specifically, the center of the combined fields-of-view is ideally pointed within 15° of the antisolar direction, and no more than 30° away. This is necessary for the sunshade and spacecraft to block solar photons. It also enables the solar panels (which are free to rotate about the $+Y$ axis in Fig. 3) to collect sunlight. Given the spacecraft's orbit [Gangestad et al., 2013], this means that *TESS* should advance $\sim 28°$ east in ecliptic longitude every lunar month, as it does during the Primary Mission. Focusing on a fixed field for say, 3 spacecraft orbits ($\approx$42 days), would be in tension with this requirement. In practice, another technical restriction is whether the Earth or Moon passes through *TESS*'s camera fields during a proposed pointing (see Sec. 3.6).

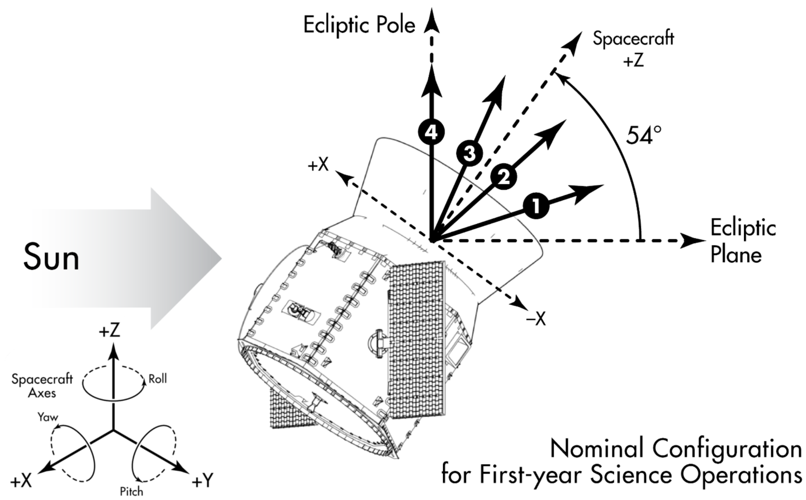

Figure 3: *TESS*'s solar panels pitch about the $+Y$ axis. The spacecraft must point so that incident sunlight is collected by the solar panels, and not the cameras. (Adapted from Orbital ATK design document)

3.2 *Our proposed pointing strategies*

For simplicity we chose to study one-year plans for an Extended Mission, i.e., plans for Year 3 of the TESS mission. (Later in this report we remark on some possible implications of our study for additional years of an Extended Mission.) Given the constraints outlined in Sec. 3.1, we selected the following options for detailed study:

Option 1. `POLE`: Focus on one of the ecliptic poles, arbitrarily chosen to be the north ecliptic pole for concreteness. Note that the geometry of *TESS*'s lens hood still suppresses incoming sunlight in this scenario. *Justification:* maximizes the average duration of observations per star; intuitively we expected this to provide greatest sensitivity to long-period planets.

Option 2. `HEMI`: Repeat observations of one of the two ecliptic hemispheres in a manner similar to the Primary Mission, arbitrarily chosen to be the northern ecliptic hemisphere for concreteness. In this scenario we could take the opportunity to shift the longitudes of all sectors by an amount that would enable TESS to cover the gaps that were left during the Primary Mission (the "slits" in the sky coverage between ecliptic latitudes of 6–30°). However for simplicity, we opted to observe the same longitudes as in the Primary Mission. *Justification:* similar motivation as the Primary Mission. Nice long time baseline at the North Ecliptic Pole, and broad sky coverage. Also remeasures transit times (and sharpens ephemerides) of previously detected TESS planets over most of the entire hemisphere.

Option 3. `HEMI+ECL`: Repeat observations of one of the two ecliptic

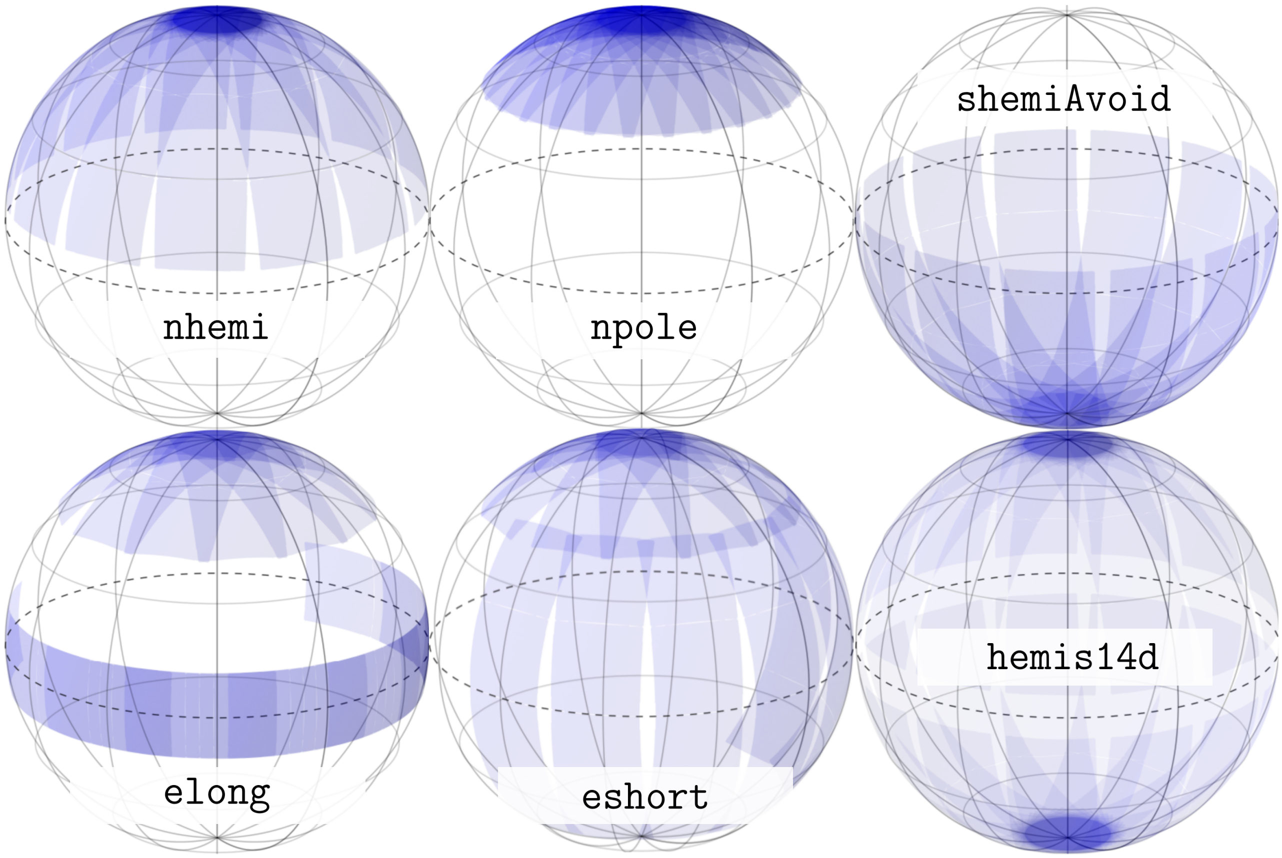

Figure 4: Proposed pointing strategies for a *TESS* extended mission, visualized in ecliptic coordinates. `HEMI`, `POLE`, `HEMI+ECL`, `ECL-LONG`, `ECL-SHORT`, and `ALLSKY`. Note for `ECL-LONG` and `ECL-SHORT` that Earth and moon crossings likely make an entire year looking at the ecliptic impractical (see Fig. 10).

hemispheres, but in this case shifting all fields 6° toward the ecliptic, such that the combined fields-of-view reach all the way from the ecliptic to the ecliptic pole. *Justification:* trades the long continuous viewing zone near the pole for greater sky coverage, and in particular, coverage of the ecliptic zone which was missed in the Primary Mission. We chose to simulate the southern ecliptic hemisphere, since the northern version of this plan would suffer more from Earth-Moon interference (cf. Table 1 in Sec. 3.6).

Option 4. `ECL-LONG`: Survey the ecliptic with 7 sectors (14 orbits) in which the long axis of the fields-of-view are oriented along the ecliptic. For the other 6 sectors, during the interval when ecliptic observations would be interrupted by Earth-Moon crossings, we focus on one of the ecliptic poles. *Justification:* covers the ecliptic, which was not surveyed at all in the Primary Mission. Offers opportunities for follow-up of K2 discoveries. Minimizes Earth-moon interference.

Option 5. `ECL-SHORT`: Survey the ecliptic and also cover a large fraction of the rest of the ecliptic hemisphere. For 7 sectors we observe the ecliptic but with the *short* axis oriented along the ecliptic, and the long axis reaching up to higher latitudes. The remaining 6 sectors are focused on the ecliptic pole, as in `ECL-LONG`. *Justification:* similar to `ECL-LONG`, but with more overlap between this year and the Primary Mission to allow for improved transit ephemerides and better ability to follow-up on previous discoveries.

Option 6. `ALLSKY`: Cover both northern and southern ecliptic hemispheres in a single year, by alternating between the hemispheres every 13.7 days. *Justification:* rapid coverage of the entire sky, allows follow-up of almost all previously detected TESS objects and refined ephemerides.

Although these 6 seemed like good options for further study and direct comparison, there are many other possibilities that may be of interest that were not studied in detail, in order to keep the scope of this report manageable. Among these other possibilities that were considered but not studied are

- The `POLE` strategy applied to the south ecliptic pole rather than the north (we do not expect major differences).
- The `HEMI` strategy applied to the southern ecliptic hemipshere rather than the northern (we do not expect major differences). Similarly, the `HEMI`strategy, but rotated about the ecliptic polar axis by 12° in ecliptic longitude.
- The north/south inversion of `HEMI+ECL`, which is more strongly affected by Earth/Moon crossings (see Sec. 3.6).
- A full year spent observing the ecliptic. It became clear that such a plan would suffer from Earth/Moon crossings for a substantial fraction of the year. We show the outage as a function of time in Fig. 10.
- Alternate between northern and southern ecliptic poles every 13.7 days. This would be similar to `ALLSKY` but would focus on the poles rather than the entire sky. It would sacrifice sky coverage (and ability to refresh ephemerides over the whole sky) in return for longer-duration observations for a typical star.
- Hybrid strategies that change from month to month. For instance, in the `HEMI` scenario, during a month when the Earth or Moon crosses through the field of a camera pointed close to the ecliptic, we could tilt all the cameras away from the ecliptic as in the `POLE` scenario.

3.3 Metrics by which we compare pointing strategies

We assess extended missions based on the risks and opportunities they present, as well as through their performance on select technical and science-based criteria. These criteria are organized following an approach originally outlined by Kepner and Tregoe [1965]. Summarizing them in list form:

Technical musts: Cameras anti-sun? Solar panels collecting sunlight?

Technical wants: Duration of each sector $<$ 28 days? Earth/Moon crossings? Zodiacal background? Scattered sunlight off lens hood?

Metrics in exoplanet science:

- number of newly detected planets (from 2-minute cadence fixed-aperture target stars, colloquially 'postage stamps', as well as 30-minute full frame images – both independently and combined);
- number of new long-period planets (which may be detected through long period coverage, or by follow-up on single-transit events);
- number of new habitable-zone planets;
- number of new planets with "characterizable" atmospheres;
- number of newly detected planets with bright host stars;
- number of stars with transiting planets detected in the Primary Mission for which the Extended Mission reveals an additional transiting planet (usually long-P companions to short-P transiting planets);
- ability to improve transit ephemerides for previously detected transiting planets;
- ability to observe more transits over a longer baseline to enable searches for transit-timing variations.

These metrics were chosen for their apparent importance as well as our ability to quantify them with simulations. Of course there are other considerations that may be very important but are more difficult to quantify:

- Prospects for altering target allocation weights between {white dwarfs, known planet-hosts, candidate planet-hosts, circumbinary & circumprimary planets, open clusters, evolved stars (notably to detect asteroseismic oscillations), dwarf stars later than M7, stars with well-measured properties, ...}.

- Prospects for observations relevant to stellar astrophysics, many of which may overlap with exoplanetary science. For instance, we may wish to try and measure a large sample of stellar rotation periods, or allocate a larger fraction of the data mass for short-cadence asteroseismic targets. We may also wish to observe optical/near-IR variable targets across the sky, in particular pulsating stars (Cepheids, RR Lyrae, Delta Scuti, slowly pulsating B stars), eruptive stars (protostars, giants, eruptive binaries, flare stars), cataclysmic variables (dwarf novae, novae, supernovae), rotating variable stars (deformed by ellipsoidal variations, showing variability from stellar spots or magnetic fields), and eclipsing binaries. Long-term observations of starspot modulation can be used to characterize long timescale stellar activity cycles.
- Prospects for solar-system science, such as observeations of main belt asteroids and the brightest near Earth asteroids.
- Prospects for extragalactic astronomy and high energy astrophysics; for instance, gathering light curves of variable active galactic nuclei.

Regarding opportunities and risks, the following need to be considered:

Opportunities:

- What's best on a > 1 year horizon for planet detections? For instance, if it were known in advance that *TESS* would continue operations for several additional years (or even 10 years), would such knowledge affect the optimal choice of the immediate one-year plan?
- Ability to move targets detected in FFIs to PSs in extended mission
- Shorten the cadence of FFIs & lengthen the cadence of 'target' stars.
- *TESS as follow-up mission:* ability to observe *CoRoT* objects; ability to observe *Kepler* field (key benefits in broader science wants above); ability to observe *K2* fields (follow-up *K2* few-transit objects); ability to observe targets previously monitored by ground-based surveys.
- *Follow-up for TESS:* potential for *JWST* follow-up? Potential for *CHEOPS* follow-up? Ability to get *TESS* photometry contemporaneously with ground-based observations? Ability to observe from both North and South hemispheres on Earth?
- Impact on Guest Investigator program?

Risks: Risk of spacecraft damage? Risk of not meeting threshold science (to be defined)? Risk of excessive false positives, for instance from crowding? Would partial instrument failure in primary mission make this scenario infeasible? Would reduced precision (from aged CCDs, worse pointing accuracy, or other mechanical sources) invalidate this scenario? Risk of planet detection simulation over or under-estimating planet yield?

3.4 *Description of planet detection model*

Sullivan et al. [2015] (hereafter, S+15) developed a simulation of *TESS*'s planet and false positive detections based on the spacecraft and payload design specified by Ricker et al. [2014]. We adapt this simulation for extended mission planning. With our additions, we can change where *TESS* looks in additional years of observing while holding fixed all other mission-defining parameters. Our approach is then to run our planet detection simulation for each plausible pointing strategy, and to compare the relative yields of detected planets. This lets us compare Extended Mission scenarios with one another and with the Primary Mission.

Background on synthetic catalogs: *TESS* is sensitive to sub-Neptune sized transiting planets orbiting M dwarfs out to $\lesssim$ 200pc and G dwarfs out to $\lesssim$ 1kpc (S+15, Sec. 2.3). It is sensitive to giant planets and eclipsing binaries across a significant fraction of the galactic disk. With this sensitivity in mind, the stellar catalog we 'observe' in our planet detection simulation is drawn from the output of TRILEGAL, a population synthesis code for the Milky Way [Girardi et al., 2005]. S+15 made some modifications to the catalog, notably in the M dwarf radius-luminosity relation, to better approximate interferometric stellar radii measurements. We retain these modifications; the modified TRILEGAL stellar catalog shows acceptable agreement with observations[7], specifically the Hipparcos sample [Perryman et al., 1997, van Leeuwen and Leeuwen, 2007] and the 10pc RECONS sample [Henry et al., 2006].

[7] Looking closely at the radius-luminosity relations, we do see non-physical interpolation artifacts. These outliers are visible in Figs. 6 and 7 below, but are a small enough subset of the population that we ignore them for this work.

With a stellar catalog defined, we populate the stars in the catalog with planets based on occurrence rates derived from the *Kepler* sample. We use rates Fressin et al. [2013] found for planets orbiting stars with $T_{\rm eff} > 4000$K and those that Dressing and Charbonneau [2015] found for the remaining M and late K dwarfs.

Detection process: We then simulate transits of these planets. Assuming the transit depth and number of transits are known, we use a model of *TESS*'s point spread function (PSF) to determine optimal photometric aperture sizes for each postage stamp star (*i.e.,* we compute the noise for all plausible aperture sizes, and find the number of pixels that minimizes this noise). With the aperture sizes and noise corresponding to a given integration time known, we compute a signal to noise ratio for each transiting object. Our model for planet detectability is a simple step function in SNR: if we have two or more transits and SNR > 7.3, we rule it as 'detected', otherwise it is not detected[8]. Our model for *TESS*'s photometric precision is described by S+15 and shown in Fig. 8.

[8] The value of this threshold is chosen to ensure that no more than 1 statistical false positive is present in the 'detections' from 2×10^5 target stars. Observing a greater number of stars, for instance in full frame images, should require a higher threshold value to maintain the same condition. We discuss this in Sec. **??**.

Assumptions of SNR calculation: Our approach to computing SNRs for each transiting object is not time-resolved. In other words, we are not simulating every 2 second CCD readout, stacking those hypothetical readouts into 2 minute cadence postage stamps and 30 minute full frames, and then reducing simulated light curves.

Our calculation is simpler. We assume perfect period-recovery, phase folding, and identical conditions between transits. We also assume that we observe a constant transit depth, which is diluted by binary companions and background stars in the same manner between transits. Our approach is then to simply tally the number of *TESS* fields a given host star falls within, which corresponds to a known total observing baseline. Assuming random orbital phasing, we then compute the number of transits *TESS* observes for planets of any given host.

With a model PSF, we determine ideal aperture sizes (see two paragraphs above), and then obtain an accurate noise per transit (since the transit durations are known, and we assume our noise, computed first over a single hour, then bins like white-noise, *i.e.,* proportionate to the inverse square root of the time in-transit).

Coupled with the known transit signal, this gives us the SNR per transit, and then to 'phase-fold our light-curves' (light-curves which are never explicitly computed point-by-point) we just[9] multiply the SNR per transit by the square root of the number of transits observed.

[9] We actually take a quadrature sum of both transit and occultation signals, but this is negligible for planets. It only matters for the case of eclipsing binaries, which we ignore in this work.

Summarizing the relevant terms in an equation,

$$
\begin{aligned}
\mathrm{SNR}_{\mathrm{phase-folded}} &\approx \sqrt{N_{\mathrm{tra}}} \times \mathrm{SNR}_{\mathrm{per-transit}} \\
\mathrm{SNR}_{\mathrm{phase-folded}} &= \sqrt{N_{\mathrm{tra}}} \times \frac{\delta \cdot D}{\left(\frac{\sigma_{1\mathrm{hr}}^2}{T_{\mathrm{dur}}} + \sigma_v^2\right)^{1/2}},
\end{aligned} \tag{1}
$$

for δ the undiluted transit depth; D the dilution factor computed from background and binary contamination (Eq. 3); $\sigma_{1\mathrm{hr}}$ the summed noise contribution from CCD read noise, photon-counting noise from the star, a systematic $60\,\mathrm{ppm} \cdot \mathrm{hr}^{1/2}$ noise floor, and zodiacal noise; T_{dur} the transit duration, and σ_v the intrinsic stellar variability (cf. S+15 Sec 3.5). The first equation is approximate because we neglect the small contribution from occultation signals.

We have changed other aspects of this simulation since S+15 was published, and describe these changes in Sec. B of the appendix.

3.5 *Selecting target stars (and full frame images)*

For the Primary Mission, *TESS*'s short cadence (2 min) targets will be drawn from a subset of the *TESS* Input Catalog. The prioritization statistic that the mission will use in this selection has yet to be explicitly defined.

Regardless, we know that for *TESS* to detect small transiting planets it should observe stars that are small and bright. For this work, we define a simple statistic, `Merit`, proportional to the SNR we should expect from an arbitrarily sized planet orbiting any star:

$$\texttt{Merit} \equiv \frac{1/R_\star^2}{\sigma_{\text{1-hr}}(I_c)/\sqrt{N_{\mathrm{obs}}}}\,, \tag{2}$$

where $R_\star$ is the radius of the star in question, $\sigma_{\text{1-hr}}$ is the relative precision in flux measurements over one hour of integration time, taken from an empirical fit to Fig 8, I_c is the Cousins band I magnitude *TESS* observes for the star (or more precisely, the star system) and N_{obs} is the number of observations the star receives over the course of the mission. For multiple systems, we use the radius of the planet host for $R_\star$, and the combined flux from all companion stars to compute the system's I_c magnitude.

We evaluate `Merit` for all the star systems in our modified TRILEGAL catalog, and then choose the best 2×10^5 as target stars to be observed at 2 minute cadence. Target stars selected in this manner are shown in Fig. 5. We take the next-best 3.8×10^6 stars and observe them at 30 minute cadence to simulate full frame image detections. This statistic is simpler than the procedure outlined in Section 6.7 of S+15 and it produces a nearly identical population of target stars (shown in Fig 6). Our approach for full frame image simulation is different from that of S+15, and we justify it further below.

We generalize this statistic to extended missions as follows: over an entire mission, the total number of observations a star receives is the sum of its observations in the primary and extended missions: $N_{\mathrm{obs}} = N_{\mathrm{primary}} + N_{\mathrm{extended}}$. If $N_{\mathrm{extended}} = 0$ for a given star, then do not select that star as a target star in the extended mission. Else, compute its `Merit` (Eq. 2) weighted by $N_{\mathrm{obs}} = N_{\mathrm{primary}} + N_{\mathrm{extended}}$. In this manner stars that are observed more during the primary mission are more likely to be selected during the extended mission.

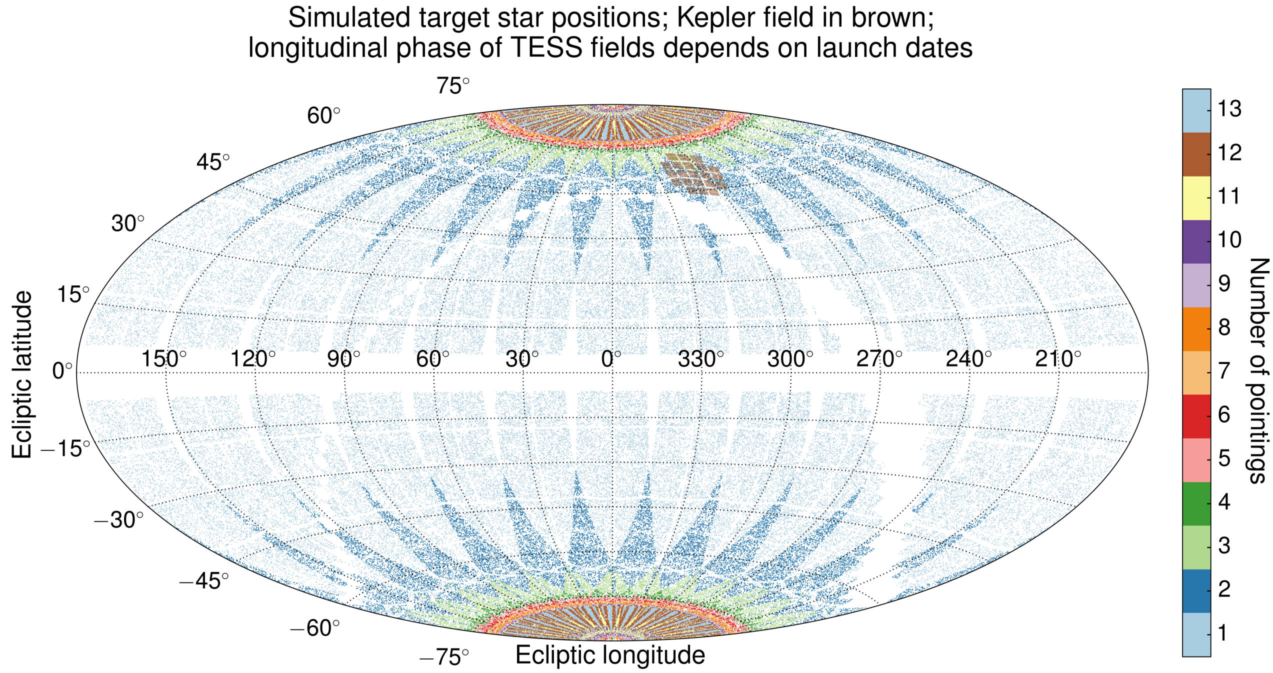

Figure 5: Selected target stars in the primary mission. Their density increases towards the poles because of the $\sqrt{N_{\rm obs}}$ weight in selection. Dead space on the CCDs creates 'gaps' in the continuous viewing zones.

Alternative prioritization approaches: It is worth emphasizing that our scheme for selecting target stars for an extended mission does not make use of any information on whether candidate transit events were observed during the primary mission. If a star were observed at short cadence for an entire year, and no candidate events were found, it may be more sensible to disregard that star in the Extended Mission in favor of stars that have never been observed at short cadence – particularly those with candidate events that were detected in the Primary Mission full-frame images. These and related concerns are discussed further at LINK!.

More abstractly, the procedure of simply applying Eq. 2 attempts to select a stellar sample that will yield the most small transiting planets around the brightest stars. An alternative approach would be to select stars that will give the most relative benefit in 2 minute postage stamps over 30 minute cadence observations. This 'relative benefit' could be a function of improved transit detectability, or perhaps improved capacity to resolve ingresses and egresses.

For purposes of transit detection, the difference between 2 and 30 minute cadence matters most when transits have short durations – in other words for small stars, and for close-in planets. Switching to this alternative approach would consequently bias us even more strongly towards selecting M dwarfs. We already select almost every M dwarf

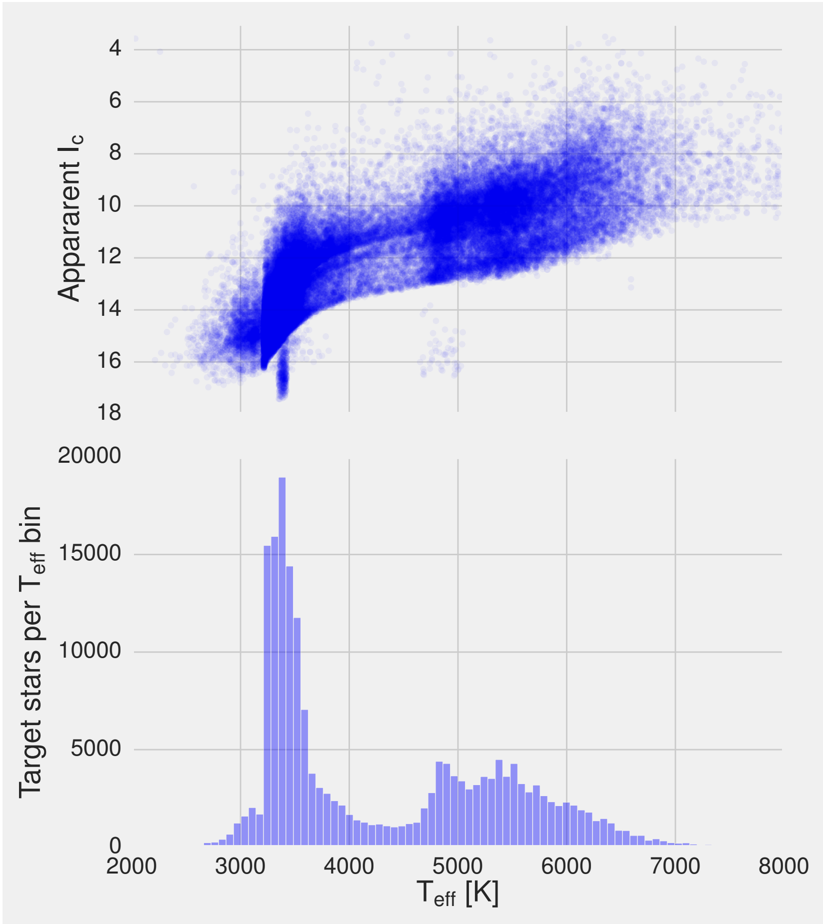

Figure 6: Replica of Figure 17 from S+15. Target stars are selected as the best 2×10^5 stars according to `Merit` $\equiv \sqrt{N_{obs}}(1/R_\star^2)/\sigma_{1\text{-hr}}(I_c)$. The top subplot shows 1 in 10 stars. This simple model could inform the target selection to be performed on the *TESS* Input Catalog. The lower histogram is bimodal, selecting heavily for M dwarfs, and selecting more F and G dwarfs than K dwarfs. This shape arises from the combined $1/R_\star^2$ and $1/\sigma_{1\text{-hr}}(I_c)$ weights: the fact that the minimum falls around K dwarfs occurs because of both a Malmquist bias (there are more F than K stars of comparable brightness in our catalog from which to select) as well as a corresponding dip in the TRILEGAL (& observed) V-band luminosity functions (see S+15 Figure 5).

Outliers visible in the upper scatter-plot are non-physical, possibly artifacts from S+15's Padova-to-Dartmouth interpolation as they tend to have greater masses than all other stars on the main sequence. They are less than 1% of the target stars; we ignore them in order to proceed.

with $I_c < 14$. The limiting I_c magnitude for detecting $R_p > 4R_\oplus$ planets with *TESS* is ~ 16, which is where we see the dimmest stars in Fig. 6.

Additionally, the procedure of applying Eq. 2 and assuming that it will maximize the number of small planets that *TESS* will detect about bright stars ignores the functional dependence of planet occurrence rates on stellar properties. For instance, should we prioritize target stars that are metal-rich? Metal-rich stars demonstrably have more giant planets within *TESS*'s period sensitivity than metal-poor stars [Fischer and Valenti, 2005, Johnson et al., 2010]. The question of whether this correlation extends to sub-Neptune radius planets is somewhat contested, but for instance Wang and Fischer [2015] used a sample of KOIs and found that the planet occurrence rates of (gas dwarf) planets are $1.72^{+0.19}_{-0.17}$ ($2.03^{+0.29}_{-0.26}$) higher around metal-rich than metal-poor stars. Note that in this usage, 'terrestrial' means $R_p < 1.7R_\oplus$, $1.7R_\oplus < R_p < 3.9R_\oplus$ – and a caution is that they only

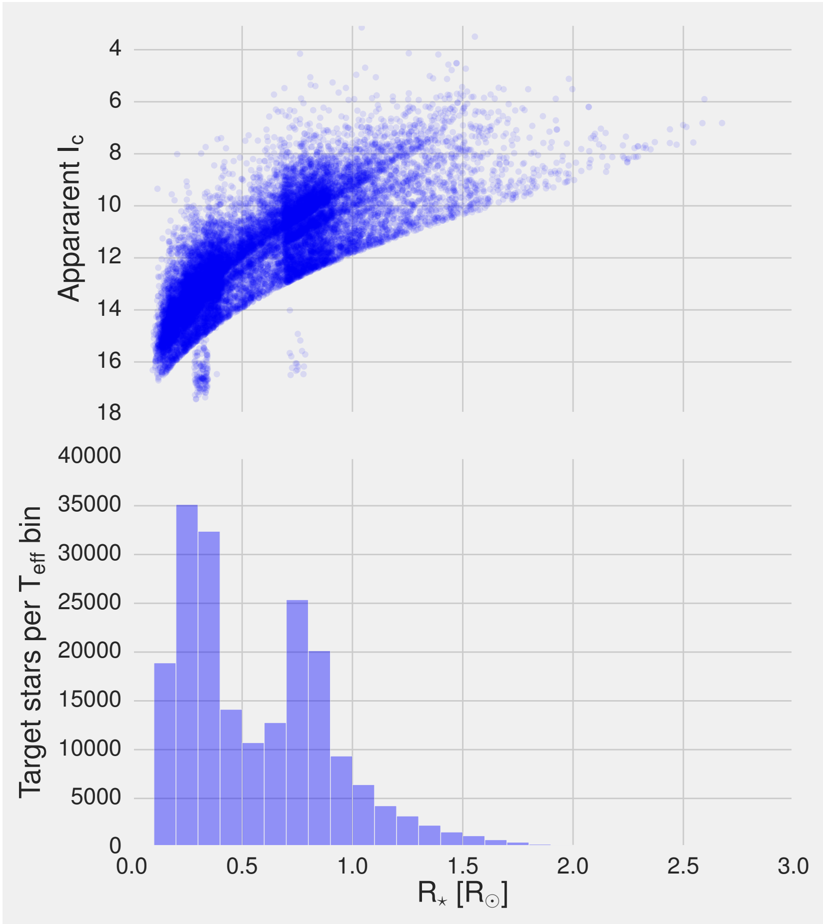

Figure 7: Same as Fig. 6, but as a function of stellar radius. $1/R_\star^2$ selection weight clearly visible, along with the same outliers.

studied solar-type stars (4800 K $< T_{\rm eff} <$ 6500 K).

A more robust approach for *TESS*'s target selection might take these kinds of results into account probabilistically. For instance, Kipping and Lam [2016] note that the probability of short-period transiters having additional transiting outer companions is functionally dependent upon the properties of the short period transiters – for instance their orbital periods and radii. They navigate the optimization problem using artificial neural networks (ANNs) trained to select for features that improve the probability of detecting transiting outer companions. *TESS* might benefit from a similar approach in target selection.

Alternative prioritization approaches in extended missions: Our `Merit` statistic also neglects the option of an extended mission which only observes stars with known planets or planet candidates (*TESS*'s objects of interest, or those from other transit and RV surveys) at short cadence. This approach would free up a considerable portion of *TESS*'s data mass for full frame images at *e.g.*, 15 minutes rather than the current nominal 30 minutes.

Approach to full-frame images: We want to simulate the full frame image detections in a computationally tractable manner. While S+15 evaluated the phase-folded SNR for every potentially transiting object about each of the $\sim 1.6 \times 10^8$ stars in our synthetic catalog, we focus only on the stars for which *TESS* could plausibly detect a sub-Neptune planet over the 3-year mission. Most stars that *TESS* sees are too dim or too large to detect $R_p < 4R_\oplus$ planets – while we expect many giant planet detections towards the galactic plane (S+15 Fig 19), small-planet detections are nearly isotropic, since practically all occur for stars at < 1 kpc. For our purposes in this study, we argue that knowing there will be thousands of giant planet candidates is sufficiently accurate. The prospects for detecting smaller planets are more likely to help discriminate between different scenarios for the Extended Mission.

In this vein, we only simulate full frame image detections for the 3.8×10^6 highest `Merit` stars following the 2×10^5 highest `Merit` stars observed as 'postage stamps'. This number (3.8×10^6) was initially estimated based on the number of searchable stars about which we expect *TESS* to be able to detect sub-Neptune radius planets [Winn, 2013]. The detection process is then identical to that for postage stamps, except with 30 minute instead of 2 minute exposures, which increases the apparent durations and shrinks the apparent depths for transits with durations of $\lesssim$1 hour. To ensure that 3.8×10^6 stars is sufficient to include all stars about which *TESS* might detect sub-Neptune radius planets, we repeated this process for the primary mission using 5.8×10^6, 9.8×10^6 and 19.8×10^6 'full frame image' stars, and confirmed that there was no significant difference in the planet yields at $R_p \leq 4R_\oplus$ between any of the cases. Increasing the number of FFI stars, the runs yield increasing numbers of giant planets, particularly near the galactic disk. Meanwhile the number of sub-Neptune radius planets remains fixed, and thus convinces us that our simulation includes a sufficient number of target stars to be complete for sub-Neptune detection statistics.

3.6 Earth/Moon crossings

When the Earth or Moon passes through *TESS*'s camera fields they can flood the CCD pixels to their full well capacity ($\sim 2 \times 10^5$ photoelectrons). Precision differential photometry becomes impossible in any pixels that are directly hit during these crossings. Even when

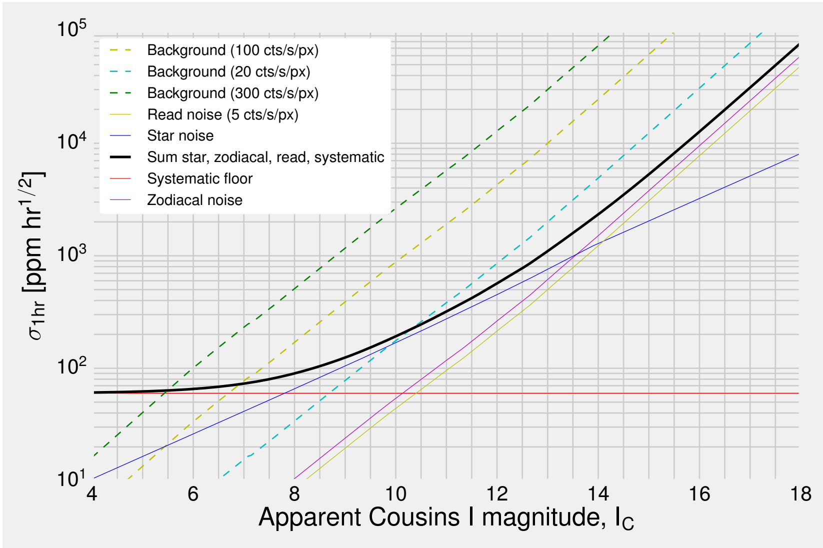

Figure 8: Relative precision in measured flux over a one hour integration time (scatter from contaminating background stars and PRF centroid offsets ignored). The noise sources described by Sullivan et al. [2015] are solid thin lines. The dashed lines exemplify noise from contaminating background flux, for instance from the Moon or Earth outside the *TESS* field, but still scattering light off the *TESS* lens hood. A dynamical 3-body simulation lets us estimate the impact lunar and Earth backgrounds have on *TESS*'s photometry. The photometric precision with which we simulate observations has additional scatter about the thick black line owing to randomly-assigned contaminating stars.

the body (the Earth or Moon) is not directly in the camera's field of view, its light scatters off the interior of spacecraft's lens hood and acts as a background source of contaminating flux across many of the cameras[10]. The Poisson noise in the number of photons arriving from the Earth or the Moon in such a scenario degrades *TESS*'s photometric performance. This can be important for field angles $\theta \lesssim 34^\circ$ (see Fig. 26 in Sec. A of the appendix). We show a few representative background fluxes in Fig. 8. The point of this figure is that for even modest background-counts the effect of scattered light could severely reduce *TESS*'s photometric performance. For instance when the moon is 30° from the camera boresights, corresponding (Fig. 26) to a suppression of 10^{-5} from the lens hood on 1.5×10^6ct/s/px from the moon, 15ct/s/px reach the cameras. This would correspond to a $2-3\times$ reduction in photometric performance for $I_c < 11$.

[10] A detailed model for this process does not yet exist. It is intended that such a model will be developed during commissioning.

Separately from our planet detection simulation, we study the impact of these crossings in a dynamical simulation based on JPL NAIF's standard SPICE toolkit. Given a nominal launch date, this code determines *TESS*'s orbital phasing throughout its entire mission. At every time step of the three-body orbit, we calculate the distance between *TESS* and the other two bodies of interest, and the separation angles among each of the four cameras and each of the two bodies (eight angles in total). The gravitational dynamics behind this calculation treat the Earth, Moon, and Sun as point masses, and the *TESS* spacecraft as a massless test particle. The spacecraft's inclination oscillates in the simulation as it will in reality.

Taking the Earth and Moon's integrated disk brightnesses as fixed

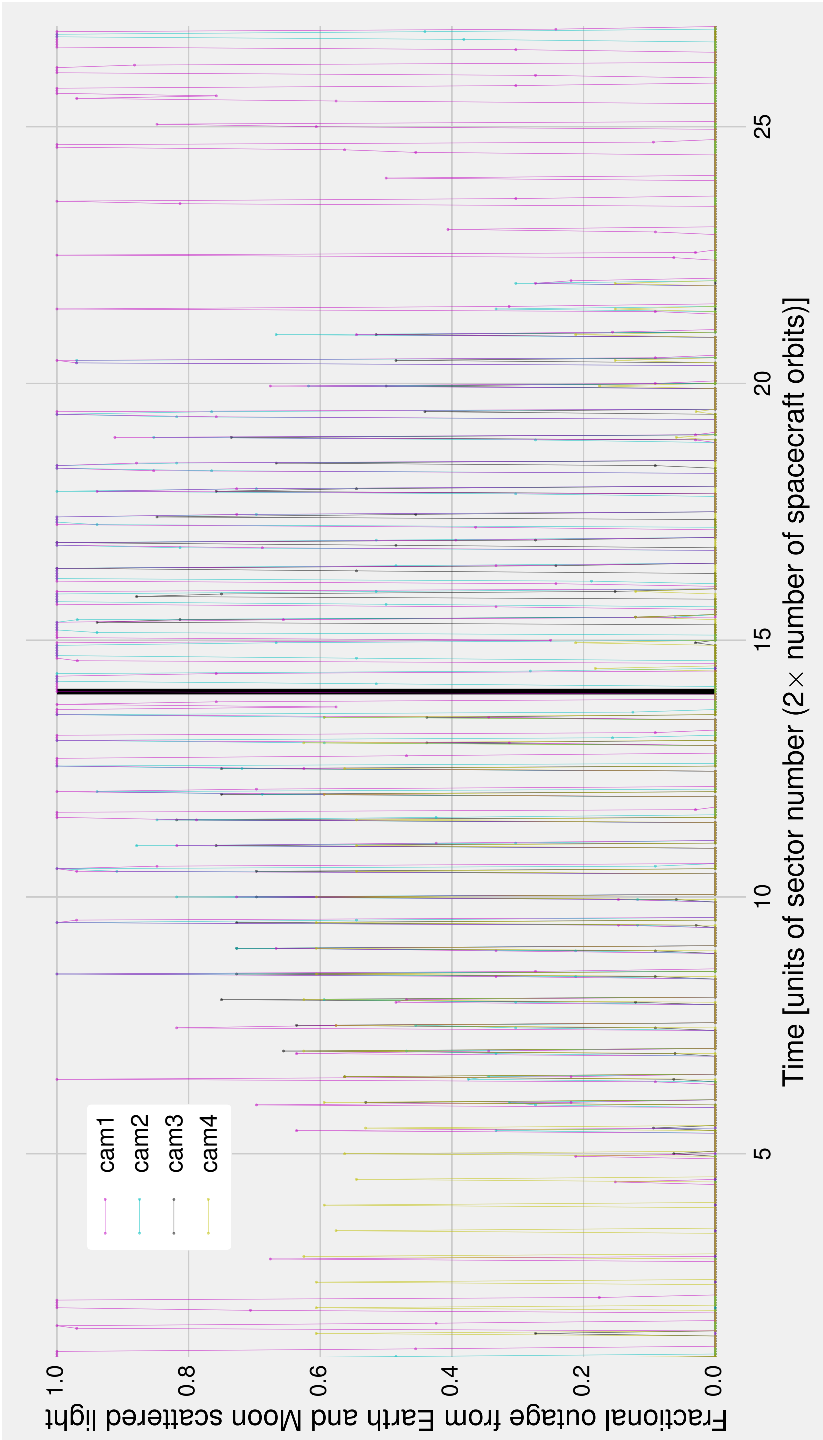

Figure 9: Fractional outage caused by Earth and Moon light either falling directly onto *TESS*'s cameras or scattering off of their lens hoods and into the lenses, as a function of time in the orbit. The first year of observations are in the southern ecliptic hemisphere. The black dividing line indicates the beginning of 'Year 2' of northern hemisphere observations. Note that the worst fractional outage per orbit is in Camera 1 (which points towards the ecliptic) over the first ~ 5 orbits of the second year. By 'fractional outage' in these plots, we mean the fraction of target stars that could be observed with $\sigma_{1\mathrm{hr}} < 10^3$ppm precision that no longer can because of Earth or Moon light. The time-step is 1/20th[th] of an orbit. The plot has 'spikes' because outage typically only occurs over a small fraction of the orbit.

values[11] we use a model for scattered light suppression from the *TESS* lens hoods (Fig. 26), to tabulate the photon flux from each of

[11] $I_{\rightmoon} = -13.5$, so the full moon delivers 1.5×10^6ct/s/px, and the Earth delivers approximately $80\times$ that amount.

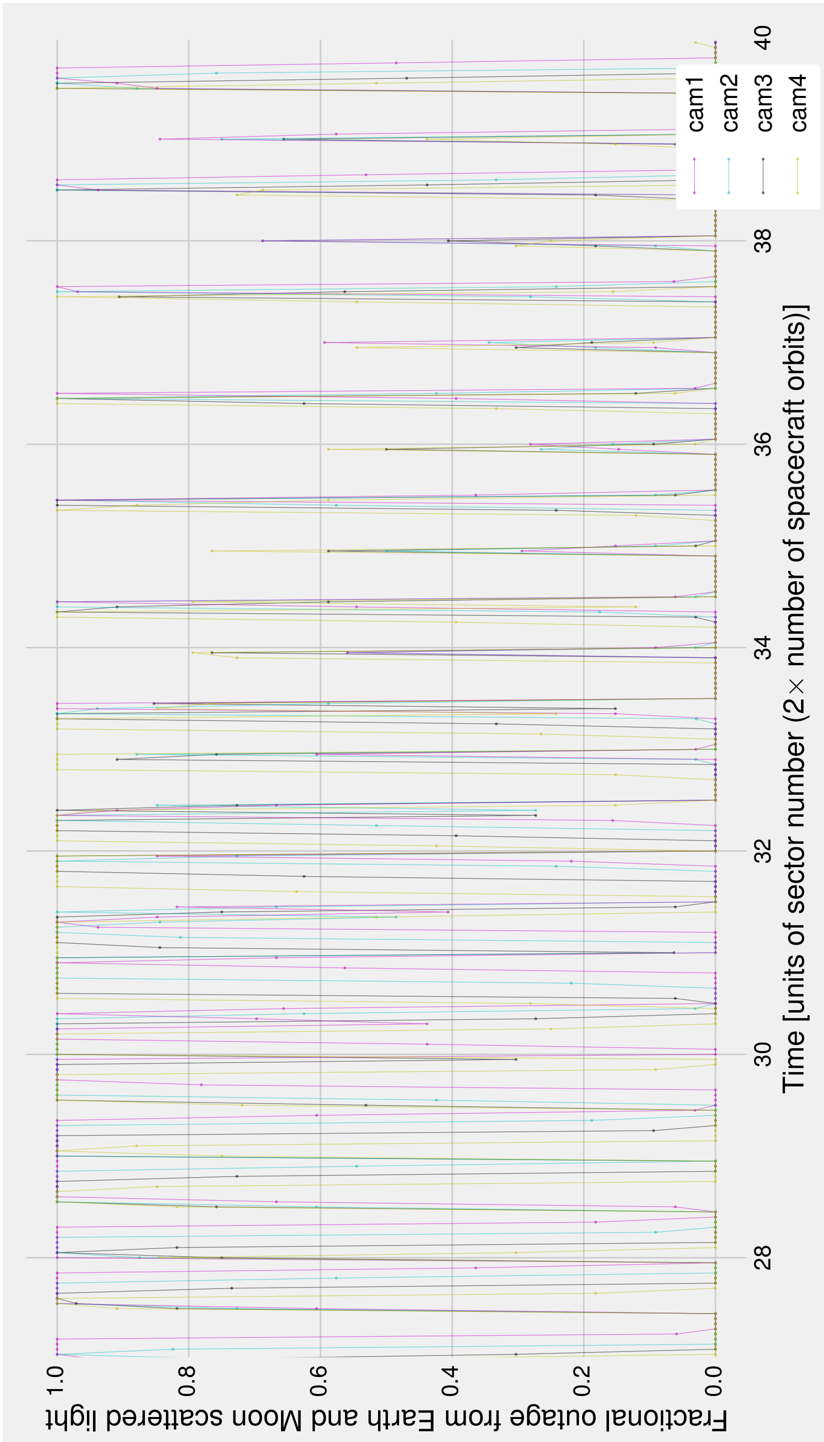

Figure 10: Same as Fig. 9, except for a hypothetical third year in which *TESS* observes the ecliptic with the cameras' long axis along the ecliptic plane. The latter half of the year experiences far less Earth and Moon interference than the first half. Considering it implausible that we would opt to sacrifice such a large fraction of our observing time ($\sim$ 50% over the first 6 months), we study the `ECL-LONG` and `ECL-SHORT` scenarios instead, as they make useful observations during the first $\sim$ 5 months (shown in Fig. 4).

these bodies onto each of the cameras throughout the orbit.

To determine the cumulative impact of these crossings on *TESS*'s observing, we ask: for each camera, what fraction of the total observing time is *TESS* unable to operate at desired photometric precision because of Earth and Moon crossings? An upper limit for what we mean by 'unable to operate at desired photometric precision' is when terrestrial or lunar flux make it impossible to observe any star in our selected target star catalog with photometric precision < 1mmag over one hour of integration time. This limit, F_{max}, is roughly

$$F_{\mathrm{max}} \approx 1000 \text{ cts/s/px} = 200 F_{\text{readout noise}}.$$

Considering *TESS*'s precision (Fig. 8), as well as the target star catalog's apparent magnitude distribution (Fig. 6), even a background of 100 ct/s/px would be a problem, since it would hinder sub-mmag photometry for all stars with $I > 10$ ($\sim$ 75% of the target star catalog). We plot the percentage of target stars that are 'lost' as a function of background counts (*i.e.*, those that could be observed at sub-mmag precision over an hour, but no longer can) in Fig. 27.

A detailed model of how these crossings impact *TESS* photometry is outside the scope of this work. That said, to account at least qualitatively for this effect in our planet detection simulation we use a simple approximation: we impose that a camera has an 'outage' if there are over $F_{\mathrm{thresh}} \equiv 300$ cts/s/px arriving from the Earth and Moon during a given exposure. We then compute the average outage time per observing sector that *TESS* suffers in each of its cameras. For instance, a given sector might have 660 hours of observing time over two spacecraft orbits, of which 220 hours might either have the Earth, the Moon, or both shining with a background $F > F_{\mathrm{thresh}}$. This would correspond to a fractional outage of 1/3. We proceed by computing the mean of this fractional outage across all 13 sectors of a given year to derive a 'mean camera outage' for each proposed pointing scenario.

As we mentioned in Sec. 3.4, our planet detection simulation is not explicitly time-resolved; it takes the ecliptic coordinates of camera fields for each orbit to compute the number of observations a given star receives over a specified mission. We decide to approximate the effect of Earth and Moon crossings by selectively omitting the closest integer number of observing sectors corresponding to the 'mean camera outage' described above. For instance, if the 'mean camera outage' was 17% of *TESS*'s observing time over a given year, we would omit the 2 (of 13) observing sectors that suffer the greatest number of lost hours, for that given camera. The relevant number of omitted sectors is shown in Table 1. While this procedure ignores the temporal nature of the 'outages' (which is shown resolved over timesteps of 1/20$^{\mathrm{th}}$ of an orbit in Figs. 9 and 10), it gives a representative sense of the cumulative impact of Earth and Moon crossings over

	Camera 1	Camera 2	Camera 3	Camera 4
Year 3 selected				
`POLE`	0	0	0	0
`HEMI`	2	1	0	0
`HEMI+ECL`	2	0	0	0
`ECL-LONG`	1	1	1	1
`ECL-SHORT`	0	1	1	0
`ALLSKY`	1	1	0	0
Year 3 omitted				
`spole`	0	0	0	0
`shemi`	1	0	0	0
`nhemiAvoid`	4	3	0	0
`elong1yr`	4	4	4	4
`eshort1yr`	1	3	4	2
`poles14d`	0	0	0	0
Primary mission				
`shemi (year 1)`	2	1	0	0
`nhemi (year 2)`	4	2	0	0

Table 1: Number of sectors (of 13 per year) 'dropped' due to the Earth and Moon crossings in both selected and omitted pointings, with those of the primary mission for reference. The method of 'dropping' fields (which omits the temporal nature of the crossings, discussed in the text) gives a representative sense of the cumulative impact of Earth/Moon crossings. `elong1yr` corresponds to a full year with the *TESS* field's long axis along the ecliptic, and `eshort1yr` corresponds to the same, but with the long axis perpendicular to the ecliptic. These scenarios are neglected because their outages are time-correlated. (see Fig. 10)

the course of a year. We discuss the impact of this approximation for the primary mission in Sec. 4.1, and for extended missions in 4.3. The summarized version is that modeling Earth/Moon crossings in this manner causes a drop of $< 10\%$ of $R_p < 4R_\oplus$ planet detections compared to the case of not accounting for the crossings at all. Given that Earth/Moon crossings typically last for a small fraction of an orbit (Fig. 9), if the timescales required for the cameras to 're-settle' after the crossings are small compared to orbital timescales, then our approach may in fact over-estimate the effect's importance.

3.7 *Summary of key assumptions and attrributes of the planet detection simulations*

- We focus almost exclusively on planets with $R_p < 4R_\oplus$.
- We assume the TRILEGAL catalog (modified to match interferometric radii, as described by S+15) is an accurate representation of the stellar neighborhood to $\lesssim$ 2kpc.
- We omit the 5% of the sky closest to the galactic disk (see Fig. 5). We expect that *TESS*'s large pixel size ($21 \times 21''$) combined with crowding near the galactic disk will cause substantial source confusion and a large astrophysical false positive rate in this area. On a practical note, TRILEGAL cannot be queried within its run-time limit for some of these fields (cf. S+15 Sec 3.1).

- We assume prior knowledge of the radii and apparent magnitudes of TRILEGAL's synthetic stars, so we can prescribe a simple prioritization statistic (Eq. 2) that we expect (but have not verified) maximizes the number of small planets we discover about bright stars[12].
- In evaluating a star's `Merit` (Eq. 2), we assume an observed magnitude for each star that comes from the sum of the flux from the star itself in addition to any companion and background stars (whose presence will not be known by the mission a priori, but which we then account for when computing 'observed' SNRs).
- We take the occurrence rate of planets as a function of radius and orbital period are from the work of Fressin et al. [2013] and Dressing and Charbonneau [2015], which are assumed to be accurate for the $P \lesssim 180$ day planets to which *TESS* is sensitive.
- The occurrence statistics of multiple-planet systems can approximated as repeated independent draws from the single-planet distributions. The orbits of planets in multiple planet systems are coplanar and stable (with period ratios of at least 1.2 between adjacent planetary orbits).
- For our instrument and noise models, we assume:
  - A point-spread function (PSF) derived from ray-tracing simulations, slightly degraded from that described by S+15, Sec 6.1 based on laboratory measurements.
  - All stars are observed at the *center* of the *TESS* CCDs. This ignores off-axis and chromatic aberrations within the *TESS* optics, and consequently ignores the angular dependence of the pixel response function (the fraction of light from a star that is collected by a given pixel). While S+15 attempted to model the field-angle dependence, we argue that the methodology used in that work was inconsistent (see appendix Sec. B), and that rectifying this approach would be complex and time-consuming. Ignoring the field-angle dependence is a simplification that may lead to loss of accuracy, but since this applies to all the scenarios under consideration, it should still be possible to *compare* the results of different scenarios without much loss of accuracy.
  - The time/frequency structure of all noise (except for stellar variability, see below) is 'white'. This means that we ignore time-correlated instrumental effects such as spacecraft jitter, thermal fluctuations, and mechanical flexure, which we expect will be at least partly mitigated by the mission's data reduction pipeline.

[12] Although it is difficult to determine accurate photometric radii, we expect that by the time *TESS* launches *Gaia* will provide parallaxes and proper motions for many *TESS* targets, allowing *TESS* to discriminate between red dwarfs and red giants for purposes of target prioritization.

  - We assume the instruments work equally well in year 3 as in years 1 and 2.
  - The assumed contributors to white noise include: CCD read noise, shot noise from stars, a systematic noise floor of 60 $\text{ppm} \cdot \text{hr}^{1/2}$, and zodiacal background. See Fig. 8 for the relative contributions of these terms as a function of apparent magnitude.
  - The noise contributions from stellar intrinsic variability are assumed to be identical to those described by S+15 Sec3.5, which uses variability statistics from the *Kepler* data computed by Basri et al. [2013]. Unlike all previously mentioned noise sources, we do not scale noise from stellar variability as $t_{\text{obs}}^{-1/2}$, since the photon flux from stars may vary over time-scales similar to typical transit durations. Instead, we assume the noise contribution from stellar variability is independent across transits, and thus scales as $N_{\text{tra}}^{-1/2}$, for N_{tra} the number of observed transits (see Eq. 1).
- For our detection model, we assume:
  - A step-function detection threshold: for $\text{SNR} \geq 7.3$, we rule transiting planets as detected, for $\text{SNR} < 7.3$, they are not detected.
  - The top 2×10^5 merit-ranked targets (Eq. 2) are observed at two-minute cadence, and the next 3.8×10^6 stars are observed at thirty-minute cadence. We use S+15 Sec. 6.8 approach to 'blurring' transits with durations $\lesssim$ 1hr, so that for longer cadence images shorter transits get shallower depths and longer apparent durations. As described in Sec. 3.5, we verify that under this assumption, our detections are complete for $R_p < 4R_\oplus$, and incomplete for Jupiter-sized planets.
  - We require ≥ 2 transits for detection. We assume the period can be recovered without ambiguity and likewise there is no ambiguity in identifying which target star is exhibiting a given transit signal.
- We do not assume any prior knowledge of previous observations that may have been performed on our stars. For instance, observing the ecliptic, we do not simulate the *TESS* -*K2* overlap.
- For Earth and Moon crossings, we assume we can drop a fixed number of orbits of observing time for the cameras that suffer most from the Earth, the Moon, or both being in *TESS*'s camera fields. We summarize this effect in Table 1. Although this ignores the time-correlated nature of the outages shown in Figs. 9 and 10,

it is sufficient for comparing detected planet yields across missions.

- We assume that we can (eventually) discriminate between astrophysical false positives (for instance background eclipsing binaries or hierarchical eclipsing binaries) and planet candidates.
- We can compute SNR with effective signal $\delta_{\mathrm{eff}} = \delta \times D$ for $\delta = (R_p/R_\star)^2$ the transit depth, and

$$D = \frac{\Gamma_N + \Gamma_T}{\Gamma_T} \quad (3)$$

where D is the dilution factor of a target star with incident photon flux Γ_T from the target star and incident photon flux Γ_N from neighboring stars (e.g., on the sky background, or binary companions).

The noise is computed by creating a synthetic image for every host star with a planet that transits above a 'pre-dilution' SNR threshold (this threshold is imposed for the sake of lowering our computational cost). This 16×16 pixel image is of the number of photoelectrons *TESS* sees from the star and its companions/background stars at each pixel of each CCD. We produce it through our PRF model, which in turn requires the host star's T_{eff} and apparent I_c. Over each image, the noise is computed for a range of possible aperture sizes about the brightest pixel (see S+15 Secs. 6.2 and 6.3), and then finally a single 'noise' for each transit is selected by choosing the aperture size that minimizes the noise.

4 *Planet detection statistics*

Using the planet detection model described in Sec. 3.4 and the target selection procedure of Sec. 3.5, we simulate three years of *TESS* observing, with for six different possibilities for the third year: `HEMI`, `POLE`, `HEMI+ECL`, `ECL-LONG`, `ECL-SHORT`, and `ALLSKY`. How many new planets do we detect, and how do their properties differ between extended missions?

4.1 *Planet yield from the primary mission*

We first examine our results for just the first two years of *TESS*'s observing, before presenting an analysis of our detected planet populations from a single extended mission (Sec. 4.2) and all six of our proposed extended missions (Sec. 4.3). Here we highlight commonalities and differences between S+15 and this work.

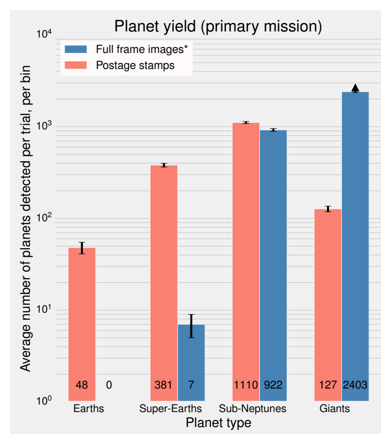

Figure 11: Mean numbers of planets detected in *TESS*'s primary mission (error bars are from Poisson fluctuations and do not account for systematic uncertainty). In postage stamp detections, the number of Earths ($R_p < 1.25 R_\oplus$), super-Earths ($1.25 R_\oplus \leq R_p < 2 R_\oplus$), sub-Neptunes ($2 R_\oplus \leq R_p < 4 R_\oplus$) and giants ($R_p > 4 R_\oplus$) is comparable to those quoted in Sullivan et al. [2015], despite modifications to our target selection procedure (Sec. 3.5). Our full frame images detections in are complete for $R < 4 R_\oplus$, and incomplete for giant planets. Here we disagree, by for instance two orders of magnitude in the super-Earth bin, with Sullivan et al. [2015] (see text).

Detected planet yield The first point of comparison is the detected planet yield from our simulation, shown in Fig. 11. The number of Earths, super-Earths, sub-Neptunes and giants we detect in postage stamps agrees with the numbers quoted by S+15, despite our modified target selection procedure. Other changes to our simulation's inputs, for instance using an as-built model of *TESS*'s PSF informed by laboratory tests (courtesy Deborah Woods) rather than the idealized PSF described in Sec6.1 of S+15, also had little impact on this final result.

However, our yields from full frame images differ markedly from those quoted in Fig. 18 of S+15. We agree with S+15 that no Earths are detected in the full frame images. However, we detect only ∼10 super-Earths by observing the $200,001^{\mathrm{st}}$ to $4,000,000^{\mathrm{th}}$ `Merit`-ranked stars at 30 minute cadence. This is two orders of magnitude less than the ∼1000 super-Earth detections claimed from FFIs by S+15. There is also a small discrepancy in FFI-detected sub-Neptunes, for which our current simulations predict that ∼1000 will be detected, while S+15 predicted ∼2000.

We empirically verified that our full frame image detections are complete for $R < 4R_\oplus$ by enlarging the number of stars observed at 30-minute cadence and seeing that the number of detected planets with radii less than Neptune did not change. We do not understand the origin of the difference between our method and S+15's, even after corresponding with P. Sullivan, but note that our results are in much better agreement with order-of-magnitude analytic arguments for *TESS*'s expected planet yield. Assuming an exponentially distributed stellar population in the galaxy and computing limiting magnitude thresholds, Winn [2013] predicted detections of $600 - 6000$ Neptunes, $24 - 300$ super-Earths, and $1 - 10$ Earth-sized planets, where the lower bounds correspond to planets detected with $\mathrm{SNR} > 10$, and the upper bounds for $\mathrm{SNR} > 7$. S+15's prediction of a total of 1500 detected super-Earths is a factor of 5 larger than these analytic estimates, while ours is in much better agreement.

Another plausibility argument that our current treatment of the FFIs is delivering more accurate results than the code employed by S+15 is that starting from the same input distribution of planets, we find a more reasonable detection bias against small planets. One should expect that the detection bias against small planets is a steep function of radius, given that $\delta \propto R_p^2$. S+15 predicted the detection of roughly twice as many sub-Neptunes as super-Earths; our current results that the ratio is closer to 5-to-1 which seems more realistic.

Properties of planets detected in primary mission We show the population properties of planets detected in postage stamps and full frame images during the primary mission in Figs. 13 and 14. In terms of the apparent planet radii R_p, orbital periods P, host star brightness, and host star $T_{\rm eff}$, we agree with the results of S+15 for the population of planets detected in postage stamps. As discussed above, we differ in the yield from full frame images. For instance, the dearth of $P < 5$ day Neptune-radius planets in Fig. 13 was observed by *Kepler* [Mazeh et al., 2016], and thus it is present in our input occurrence rates, rather than being an observational bias. It was also seen by S+15.

The differences between planets detected in postage stamps vs. in full frame images follow our expectation from our `Merit` statistic. Namely, Fig. 14 shows that at a fixed brightness, full frame image detections tend to occur at larger stellar effective temperature (and thus stellar radius). At a fixed host star radius, postage stamp detections occur around brighter stars.

Impact of earth and moon crossings on primary mission's detected planet yield During the primary mission, of the four cameras Camera 1 (closest to the ecliptic) suffers the most from earth and moon crossings. We remove 4 of its 13 'observing sectors', as noted in Table 1. This reduces the number of planet detections near the ecliptic, and is visible in the orange points of Fig. 12. In the primary mission *TESS* detects ~ 20 planets with $R_p < 4R_\oplus$ from both 2 minute and 30 minute data in each $24^\circ \times 24^\circ$ camera field nearest to the ecliptic (where each field is observed for 2 *TESS* orbits). As implemented in our simulation, Earth and Moon crossings result in fields simply not being observed, so in these cases planets orbiting stars in these fields are never detected. Considering only the primary mission, we would naively expect that dropping a total of 9 fields over the two years (again, see Table 1) would result in a loss of $\sim 9 \times 20 = 180$ planets. This agrees with what our simulations actually give: running them without accounting for Earth and Moon losses returns a mean of 2678 detected planets with $R_p < 4R_\oplus$, while running them with Earth and Moon crossings gives a mean of 2482 such planets (a loss of 196 planets, or 7% of the sub-Neptune yield).

4.2 *Planet yield from an example extended mission* (`HEMI`)

Before comparing our six selected extended mission scenarios simultaneously (Sec. 4.3), we describe the detected planet populations from a single realization of an extended mission. As an example case, we choose the `HEMI` scenario.

A sky map showing the positions of detected planets for this mission is drawn in Fig. 12. Commenting on this map, we note that:

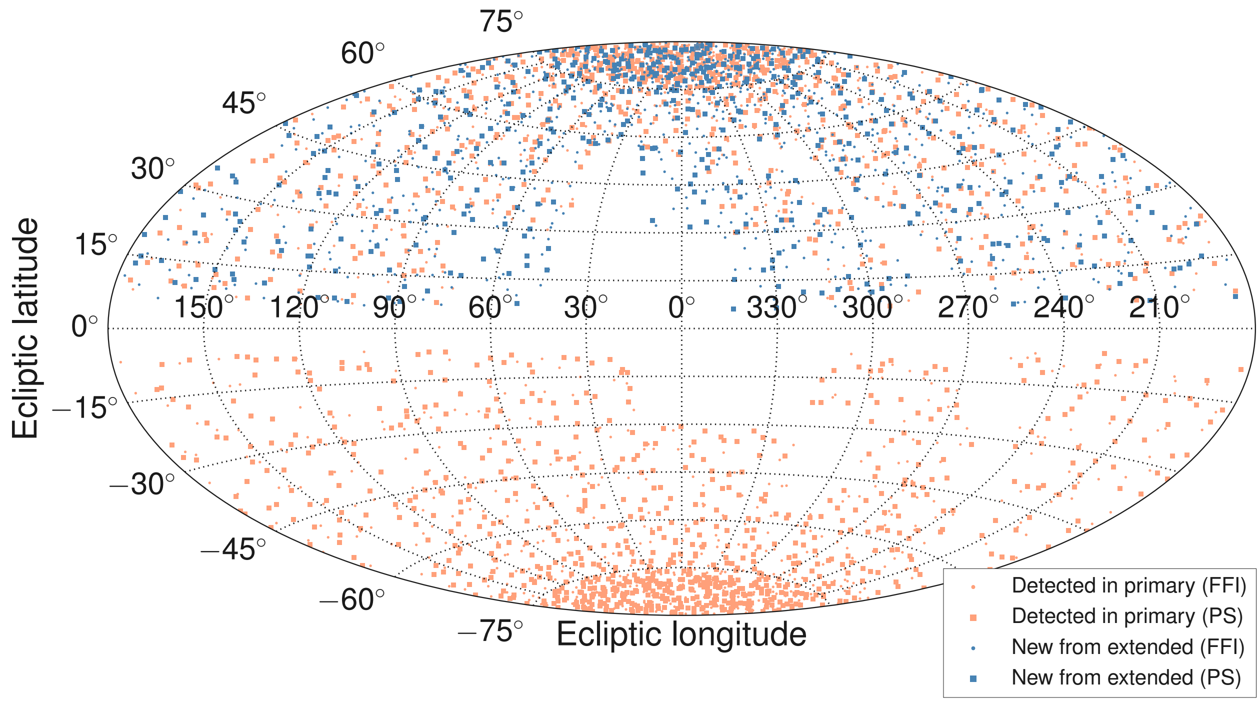

Figure 12: Positions of $R_p < 4R_\oplus$ planets detected in the `HEMI` scenario. Squares (postage stamps) and dots (full frame images) are observed at 2 and 30 minute cadence respectively. Orange denotes detection over the first two years of observing (the primary mission), and blue denotes newly detected planets from the extra third year. The 'gaps' in fields due to Earth and Moon crossings during the primary and extended missions are noted in Table 1. For instance, the field centered at $(\lambda = 330°, \beta = 18°)$ is observed in the extended but not the primary mission.

- Any planet detected in this scenario's primary mission is also detected in its extended mission. We consequently color the detected planets depending on if they are discovered in the primary mission, or whether they are detected only by virtue of the extra data collected in the Extended Mission. In our simulation, these extra observations will lead to new detections (a) because of an increased number of observed transits leading to a higher phase-folded SNR, which causes the transiting object's SNR to clear our threshold of 7.3, and/or (b) because raising the number of observed transits clears the minimum number of transits we require for detections ($N_{\rm tra} \geq 2$).
- The 'dropped' fields described in Sec. 3.6 owing to Earth/Moon crossings are visible for both the primary and extended missions in the $\lambda = (30°, 0°, 330°, 300°)$ fields.

In addition to examining the positions of the detected planets, we select and plot some of their key properties: planet radius R_p, orbital period P, apparent magnitude I_c, and effective temperature $T_{\rm eff}$. See Figs. 13 and 14. Both of these figures are visualizations from a single Monte Carlo realization of the `HEMI` scenario, and only show planets with $R_p < 4R_\oplus$. These plots clarify a few points:

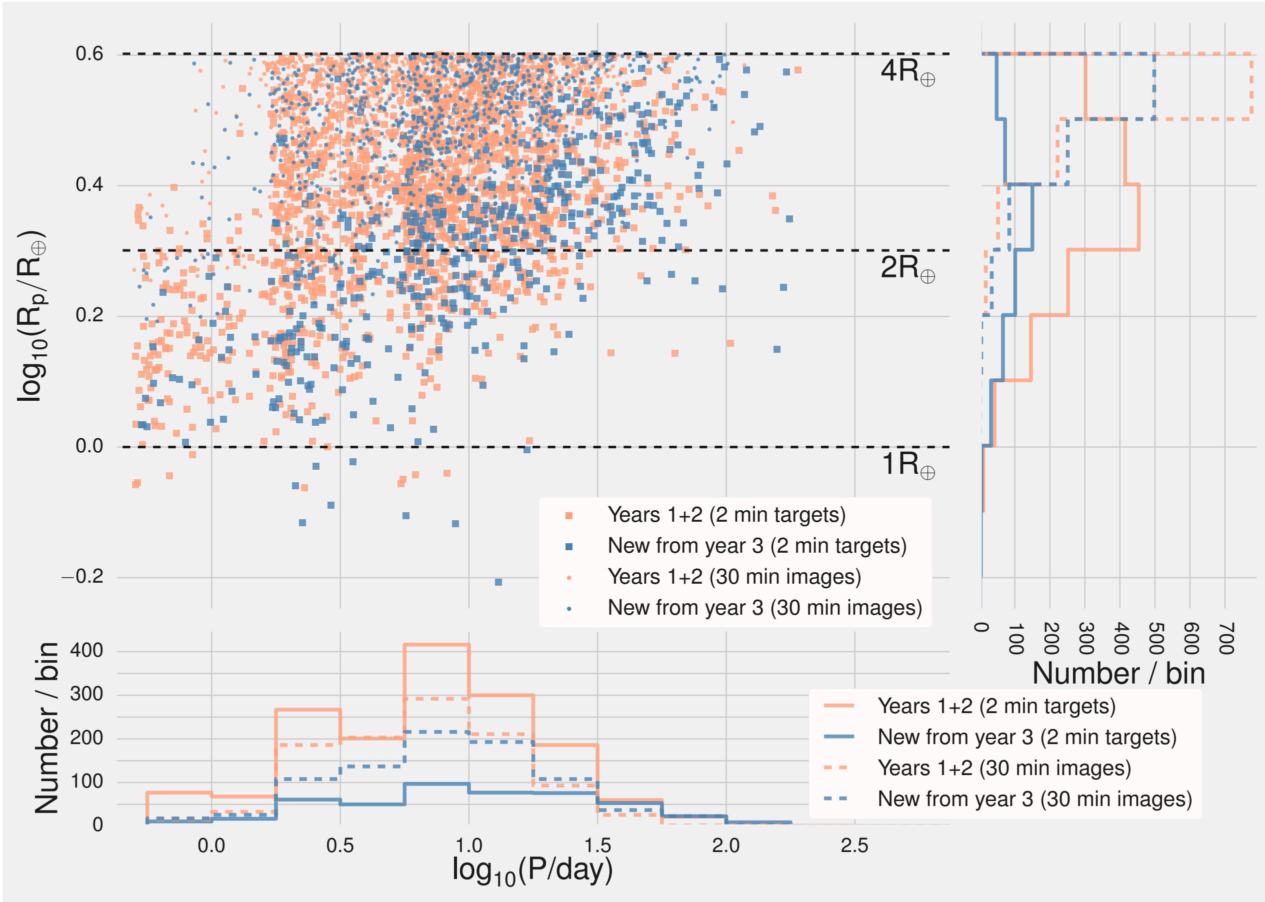

Figure 13: Radius vs period of detected $R_p < 4R_\oplus$ planets from one Monte Carlo realization of the `HEMI` scenario. At a fixed period, extended missions help us detect smaller planets; at a fixed radius, they let us probe out to longer periods. The radius histogram, and the location of all dots (rather than squares) on the scatter plot show that almost all $R_p < 2R_\oplus$ planets are detected in postage stamps, not full frame images (also shown in Fig. 11).

- At a fixed period, extended missions help us detect smaller planets; at a fixed radius, they let us probe out to longer periods. This is one of the major reasons to extend *TESS*'s observations.
- Almost all $R_p < 2R_\oplus$ planets are detected in postage stamps, not full frame images. This is an indication that the top 2×10^5 `Merit` stars are a sufficient sample to detect most of the $R_p < 2R_\oplus$ planets that *TESS* can detect.
- Postage stamp detections are biased towards M dwarfs. Per Fig. 6, this is largely because our selection procedure chooses many M dwarfs.
- For a given effective temperature, full frame images detect planets about dimmer stars. Projecting the FFI detections onto apparent I_c magnitude (Fig. 14, right panel), the median brightness of stars with planets detected from FFIs is actually greater than the median brightness of planets detected from PSs. This is because these

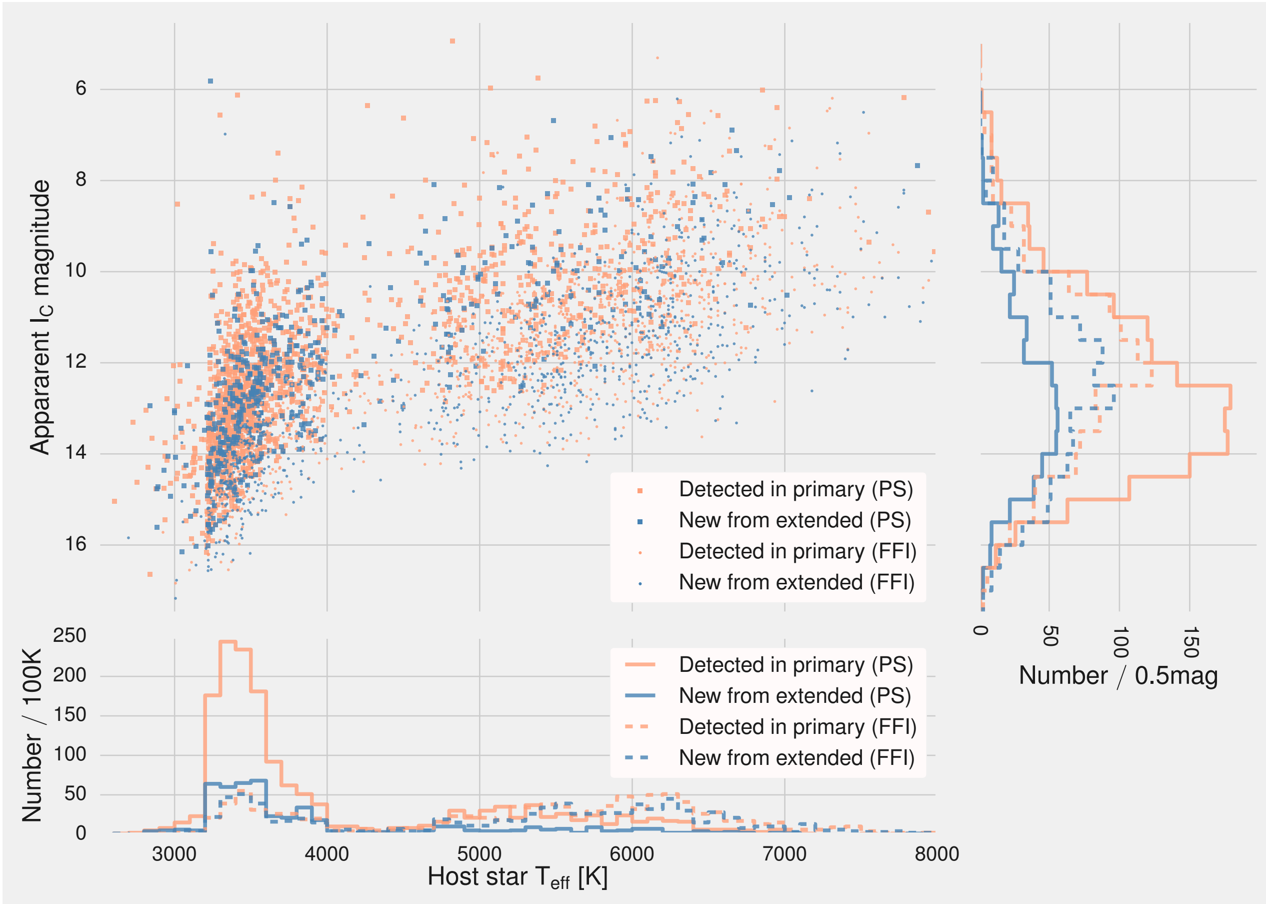

Figure 14: Apparent Cousins I magnitude plotted against effective temperature for $R_p < 4R_\oplus$ planets detected from one Monte Carlo realization of the `HEMI` scenario. Postage stamp (PS) detections are biased towards M dwarfs in part because of our selection procedure. For a given effective temperature, full frame images (FFIs) are taken of dimmer stars.

detections are about stars with radii that, on average, are greater than those from postage-stamp detections.

There are a few other statistics that interesting for purposes of characterizing the value of this extended mission – how many new planets do we detect? How many are at long orbital periods? How many are in habitable zones? We respond to these questions in Sec. 4.3, in particular showing our detected planet yields in Fig. 15.

4.3 *Comparing planet yields from all extended missions based on new planet detection metrics*

To compare extended missions in terms of planet detection statistics, we focus on the subset of all detected planets that are *newly* detected from each extended mission. These may come from stars that were not observed at all in the primary mission (notably for scenarios such as `ECL-LONG`), or they may also come from transiting planets that were observed in the primary mission with SNR < 7.3, or from planets that were single-transiters in the primary mission (we require $N_{\rm tra} \geq 2$) for detection. With this in mind, for each extended mission scenario we ask the following questions:

1. $N_{\rm new}$: How many new planets do we detect?
2. $N_{\rm new,P>20d}$: How many of these new planets are at long orbital periods, for instance $P > 20$ days?
3. $N_{\rm new,HZ}$: How many are in the habitable zone?
4. $N_{\rm sys,extra\ planets}$: In how many systems in which at least one planet was detected during the primary mission do we find extra planets in the extended mission?
5. $N_{\rm new,atm}$: How many new planets do we find that are amenable to atmospheric characterization (defined below by Eq. 4)?
6. $N_{\rm new,new\ stars}$: How many of the new planets come from stars that were not observed in the primary mission, vs.
7. $N_{\rm new,SNR \vee N_{tra}}$ stars that were observed, but either did not have enough transits or a high enough SNR to result in a detection.

For each Year-3 scenario, we compare these numbers to the corresponding numbers from the Primary Mission as well as to the other 5 scenarios for Year 3. We show the results of our simulations in Fig. 15. The first point to notice is that for all but one of the new planet detection metrics ($N_{\rm new}$, $N_{\rm new,P>20d}$, $N_{\rm new,HZ}$, $N_{\rm sys,extra\ planets}$, $N_{\rm new,atm}$, $N_{\rm new,SNR \vee N_{tra}}$) the yields between extended missions vary by less than a factor of two. The exception is in $N_{\rm new,new\ stars}$, in which `ECL-LONG` detects roughly twice as many planets orbiting never-before-observed stars as any other proposed mission.

The second point is on the absolute yields of new planets: postage stamp observations find $\mathcal{O}(500)$ new planets, relative to the primary mission's $\mathcal{O}(1500)$. Full frame image observations find $\mathcal{O}(800)$ new planets, relative to the primary mission's $\mathcal{O}(900)$. All extended missions find $\mathcal{O}(1300)$ new planets, relative to the primary mission's $\mathcal{O}(2500)$. We discuss these results – the rough invariance of the number of new planets to different pointing scenarios, and the essential contribution of FFIs – further in point #1 below.

Skimming the bottom panel for which missions are highlighted in green when accounting for both PSs and FFIs, we see that `POLE` and `ALLSKY` are the 'superlative-winning' missions in terms of detected planet statistics: considering both PSs and FFIs, `POLE` places top-2 in 5 of 8 relevant categories, and `ALLSKY` does the same in 6 of 8. They

	nhemi-ps	npole-ps	shemiAvoid-ps	elong-ps	eshort-ps	hemis14d-ps
N_{uniq}	2051	2219	2051	2114	2127	2130
N_{new}	499	616	482	530	472	584
N_{pri}	1544	1543	1547	1557	1552	1543
$N_{\text{new,P>20d}}$	137	153	119	118	108	176
$N_{\text{pri,P>20d}}$	214	210	213	216	215	216
$N_{\text{new,HZ}}$	102	108	101	95	94	128
$N_{\text{pri,HZ}}$	196	201	200	208	202	200
$N_{\text{sys,extra planets}}$	62	54	59	38	53	82
$N_{\text{new,atm}}$	11	7	19	19	21	17
$N_{\text{pri,atm}}$	97	102	100	99	104	98
$N_{\text{new,new stars}}$	29	37	70	193	110	20
$N_{\text{new,SNR}\vee\text{N}_{\text{tra}}}$	471	580	411	337	362	564

	nhemi-ffi	npole-ffi	shemiAvoid-ffi	elong-ffi	eshort-ffi	hemis14d-ffi
N_{uniq}	1716	1682	1762	1558	1574	1776
N_{new}	785	803	846	639	744	849
N_{pri}	940	939	938	947	933	931
$N_{\text{new,P>20d}}$	116	122	114	89	110	128
$N_{\text{pri,P>20d}}$	80	82	80	80	83	80
$N_{\text{new,HZ}}$	20	16	21	12	25	18
$N_{\text{pri,HZ}}$	9	8	9	9	8	9
$N_{\text{sys,extra planets}}$	9	7	9	5	7	10
$N_{\text{new,atm}}$	3	1	5	2	2	5
$N_{\text{pri,atm}}$	7	7	7	7	7	6
$N_{\text{new,new stars}}$	35	56	90	173	61	22
$N_{\text{new,SNR}\vee\text{N}_{\text{tra}}}$	750	747	755	466	682	827

	nhemi-both	npole-both	shemiAvoid-both	elong-both	eshort-both	hemis14d-both
N_{uniq}	3767	3901	3813	3672	3701	3907
N_{new}	1284	1419	1327	1169	1216	1433
N_{pri}	2483	2482	2486	2504	2485	2474
$N_{\text{new,P>20d}}$	253	275	234	207	218	304
$N_{\text{pri,P>20d}}$	294	292	294	296	298	296
$N_{\text{new,HZ}}$	122	124	122	107	120	146
$N_{\text{pri,HZ}}$	205	210	209	217	210	208
$N_{\text{sys,extra planets}}$	71	65	67	44	61	92
$N_{\text{new,atm}}$	14	8	24	21	23	22
$N_{\text{pri,atm}}$	104	108	107	106	112	104
$N_{\text{new,new stars}}$	63	92	161	366	171	42
$N_{\text{new,SNR}\vee\text{N}_{\text{tra}}}$	1220	1327	1167	803	1045	1390

Figure 15: Detected planet metrics for six possible extended missions (values are means of 50 Monte Carlo realizations of our calculation, all for $R_p < 4R_\oplus$). *Top:* postage stamp detections, *Middle:* full frame image only detections, *Bottom:* sum of both. The best two scenarios for select statistics are highlighted in green.

N_{uniq}: number of unique planets detected over all 3 years. N_{new}: number of planets detected in year 3 that were not detected in years 1&2 (newly detected planets). N_{pri}: number of planets detected in the primary mission (years 1&2). $N_{\text{new,P>20d}}$: number of newly detected planets with orbital periods greater than 20 days. $N_{\text{pri,P>20d}}$: same as previous, but from the primary mission. $N_{\text{new,HZ}}$: number of newly detected planets satisfying $0.2 < S/S_\oplus < 2.0$ (approximate habitable zone). $N_{\text{pri,HZ}}$: same as previous, from the primary mission. $N_{\text{sys,extra planets}}$: number of systems in which extra planets are detected. $N_{\text{new,atm}}$: number of newly detected planets with SNR in transmission greater than (that of GJ 1214b)/2, as measured by *JWST* – see text. $N_{\text{pri,atm}}$: same as previous, from primary mission. $N_{\text{new,new stars}}$: number of newly detected planets that orbit stars that were not observed during the primary mission. $N_{\text{new,SNR}\vee\text{N}_{\text{tra}}}$: number of newly detected planets that were observed during the primary mission, but either (a) which had SNR < 7.3, a non-detection and/or (b) had $N_{\text{tra}} < 2$, and so would not be 'detected'.

both do well at maximizing the number of newly detected planets, while also performing well at detecting long period planets, and thus planets in their stars' habitable zones. `ALLSKY` also has the largest number of systems in which extra planets are detected.

We now discuss each metric in more depth:

1. N_{new}: we detect about as many new planets in Year 3 as we detect planets in either Years 1 or 2: roughly 1250. The worst and the best scenarios (`ECL-LONG` and `ALLSKY`, respectively) differ only by a factor of 1.2. The fact that there are so many new planets to be detected from extended observations, particularly from full frame images, and that the absolute number of new planets is roughly invariant to the spacecraft's pointing, can be understood from Fig. 16. This figure illustrates a point that was originally noted

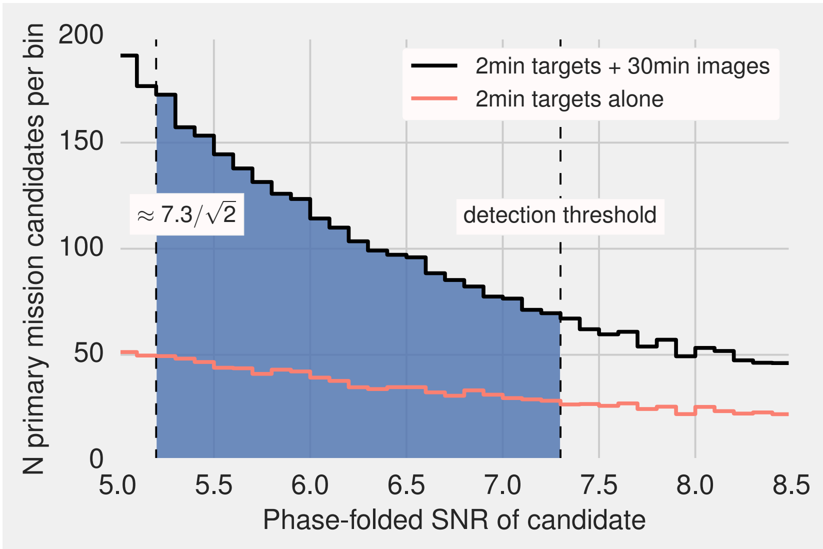

Figure 16: Histogram of phase-folded SNRs for candidate $R_p < 4R_\oplus$ planets following the primary mission (from both PS and FFI observations; values are means of 20 Monte Carlo trials). If an extended mission observes half of the sky, it roughly doubles the number of observed transits for half of the planets observed in the primary mission, enabling detection of $\approx 2316/2 = 1158$ planets (half of the blue integrated area in the plot). This coarse estimate is a similar result to our detailed calculations, and shows the value of continuing *TESS*'s observations *irrespective of where we observe.*

by S+15. The *TESS*'s Primary Mission will miss many short-period planets around bright stars, and is therefore incomplete even its intended hunting ground. For stars with $I_c > 9$, there are at least an order of magnitude more $R_p < 4R_\oplus$ transiting planets that *TESS* does not detect (Fig 22 of S+15). Our findings agree: there are a substantial number of planets just below the detection threshold, predominantly with $2R_\oplus < R_p < 4R_\oplus$ (Fig. 11). An extended mission will probe and detect this population, irrespective of where on the sky we observe. This result should hold equally well for realistic detection efficiency thresholds, and it is demonstrates that extended observations will be valuable, because *TESS* will not yet be at the point of diminishing returns for longer observations (which will happen when more observations only allow pushing out to longer orbital periods). There will still be small, short-period candidates to discover after *TESS*'s primary mission.

2. $N_{\text{new,P>20d}}$: it will be possible to detect as many new $P > 20$ day planets in one year of *TESS*'s extended mission as in both years of the primary mission. The primary mission detects about 295 such planets; `ALLSKY` and `POLE` scenarios detect similar amounts. These two scenarios are achieving the goal of long-period planet detection in slightly different ways: `POLE` maximizes the average observing baseline per star, while `ALLSKY` observes the greatest possible number of stars for longer than 40 days. The latter approach could succeed at detecting many planets (our result is that `ALLSKY` detects the most $P > 20$day planets), but it relies heavily

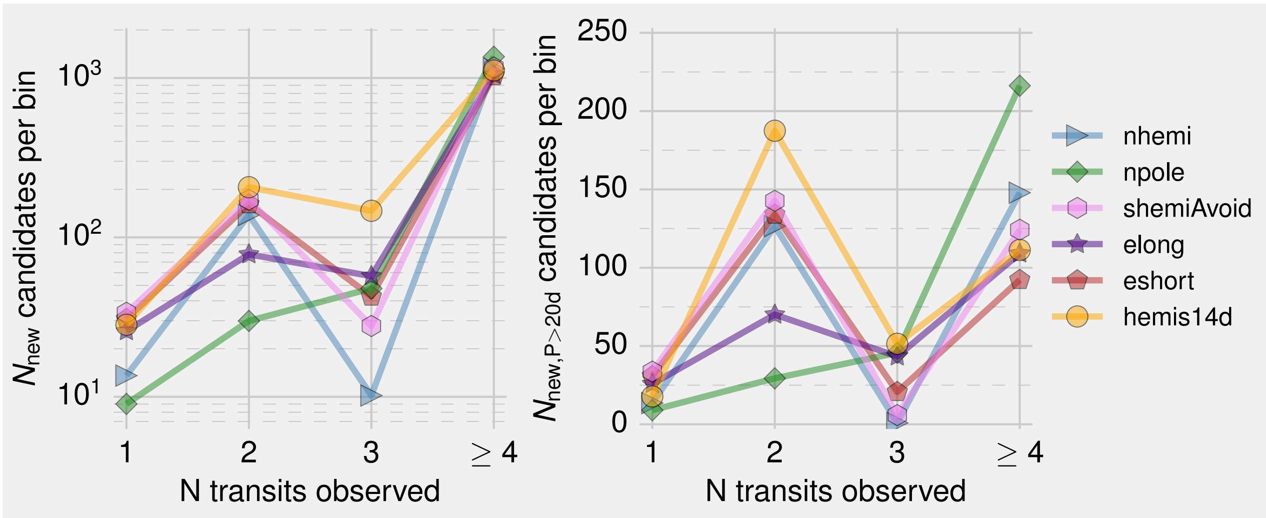

Figure 17: *Left:* Histogram of new $R_p < 4R_\oplus$ planet candidates from each extended mission as a function of the number of observed transits. Candidates are 'detected' in Fig. 15 if $N_{\rm tra} \geq 2$. *Right:* Same as left, restricted to $P > 20$ day planets. If any given scenario has a 'bump' at 2 observed transits, then that scenario depends more heavily on our assumption of being able to make detections based on only two transits. Lines between points have no physical meaning; they are intended to improve readability.

upon the assumption that we can detect planets from only two transits over the course of the entire mission, even if this means only one transit in the primary, and one transit in the extended.

This point – that the ability of the ALLSKY scenario to detect many long period planets is grounded on the assumption that two transits at high enough SNR are sufficient for detection – is made explicit in the right panel of Fig. 17. About half of the long period planets that ALLSKY finds are detected with only two transits. By way of comparison, POLE detects most of its long-period planets with $\geq$ 4 transits. This means that the POLE detections are more secure. For two-transit detections, especially those separated by a gap of a year or more in the *TESS* data, it will be difficult to be very confident in the detection, and in the derived orbital period. Experience from the *Kepler* mission showed that requiring 3 or more self-consistent transits substantially lowers the fraction of false signals [Burke et al., 2014]. In cases with a relatively high SNR per transit it is possible to confirm candidates, but with less certainty than if we had more transits in the first place.

3. $N_{\rm new,HZ}$: we approximate the habitable zone as the geometric shell around a host star in which a planet's insolation satisfies $0.2 > S/S_\oplus > 2.0$. With this approximation, the ALLSKY scenario finds the most new habitable zone planets: 146 (which is subject to the same caveats discussed above for long period planet detections). The next-best scenarios, POLE, HEMI and HEMI+ECL, all detect around 120. Relative to the primary mission's 210 detections, this means extended missions boost the number of detected habitable

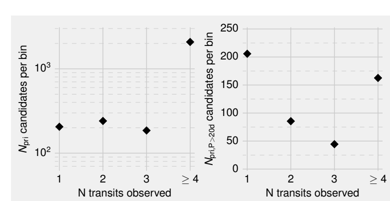

Figure 18: Similar to Fig. 17, but for the primary mission.

zone planets by a factor of ~ 1.6. For purposes of weighing the value of habitable-zone detections in deciding between missions, the result that these scenarios all detect a similar number of planets indicates that this metric will likely not 'tip the scales' in any direction.

We note in passing that $\sim 80\%$ of the habitable zone planets that *TESS* detects orbit M dwarfs with spectral classes ranging from M4 - M0, and $\sim 15\%$ of them orbit M dwarfs later than M4. We show this quantitatively in Fig. 19. Additionally, our values for the number of $0.2 < S/S_\oplus < 2$ planets from the primary mission are slightly revised from those of S+15: while S+15 quote 48 ± 7 $0.2 < S/S_\oplus < 2$ and $R_p < 2R_\oplus$ planets, we find 34 ± 5. Adopting the habitable zone of Kopparapu et al. [2013], S+15 quoted 14 ± 4 $R_p < 2R_\oplus$ planets. We find 11 ± 3. The rule of thumb that extended missions give roughly $1.6\times$ the number of new $0.2 < S/S_\oplus < 2$ habitable zone planets applies to the Kopparapu et al. [2013] habitable zone as well as $0.2 < S/S_\oplus < 2.0$. Another result shown in Fig. 20 is that the Kopparapu et al. [2013] habitable zone, which is physically motivated by 1-D radiative-convective cloud-free climate models with accurate absorption coefficients, results in roughly 3 times fewer 'habitable zone' planet detections than our ad-hoc criteria of $0.2 < S/S_\oplus < 2$.

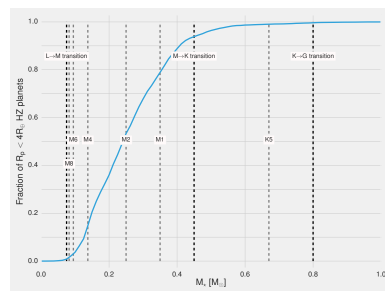

Figure 19: Cumulative distribution of $R_p < 4R_\oplus$ and $0.2 < S/S_\oplus < 2$ planet candidates from the primary mission (a proxy for the habitable zone). Boundaries of spectral classes are highly approximate, and taken from from Habets and Heintze [1981] and Baraffe and Chabrier [1996].

4. $N_{\text{sys,extra planets}}$: for how many systems do we detect extra planets? Our assumptions about multiple planet system distributions are crude – we assume independent probability draws from single planet occurrence distributions. Thus our simulated planet population does not have systems of tightly packed inner planets in realistic numbers. That said, we expect this statistic to be some indication of the information that we are not explicitly modeling, but which can be obtained from extended observations of planetary systems post-planet detection. This additional information includes improved precision on physical and dynamical parameters of the system. It also includes transit timing variations, which could be used to discover non-transiting planets as well as transiting outer companions. TTVs can also give dynamical hints for the formation history of planetary systems, for instance, discriminating between *in situ* formation and inward migration as Mills et al. [2016] argued for the Kepler 223 system.

   The most prominent feature in the results for this metric is that `ECL-LONG` detects the fewest systems with extra planets (44, which is 39% worse than the next-best). This is reasonable because `ECL-LONG` spends the most time looking at new sky, and in the process observes fewer systems that were detected in the primary

Figure 20: Scatter plot of $R_p < 4R_\oplus$ planet candidates falling in the S+15 or Kopparapu et al. [2013] habitable zones.

mission. `HEMI`, `HEMI+ECL`, `POLE`, and `ECL-SHORT` all perform similarly, detecting $\sim$ 65 such planets. `ALLSKY` detects the most, at 92. While this is still subject to the assumption of two-transit recoverability, in this case the requirement is not too strong: only 10 of `ALLSKY`'s systems with newly detected planets come from the case where the extra detected planet comes from two transits.

5. $N_{\rm new,atm}$: We define 'planets that are amenable to atmospheric characterization' to mean planets whose SNR in transmission is greater than (that of GJ 1214b divided by 2), where the latter factor of 2 gives us a sufficiently large sample to prevent Poisson fluctuations from hindering our comparisons. The relevant signal in transit spectroscopy is the ratio of the areas of atmosphere's annulus to the star's disk on the sky plane, $\delta_{\rm atm} = 2\pi R_p h_{\rm eff}/(\pi R_\star^2)$, where the effective scale height of the atmosphere $h_{\rm eff}$ is proportional to the actual scale height. Assuming that the planet is in thermal equilibrium with incident radiation from the host star, and that its atmosphere has known mean molecular weight and Bond albedo, we can compute a representative signal. The noise performance depends on the observing instrument, and could be complex if not simply dominated by shot-noise from IR photons. We circumvent such complexities via an empirical formula provided to us by Drake Deming, based on a multi-variate regression fit to detailed simulations performed by Dana Louie. This formula estimates the SNR in transmission from 4 transits observed with *JWST*'s NIRISS instrument:

$$\begin{aligned} \log_{10} \mathrm{SNR} = 2.98 \log_{10}\left(\frac{R_p}{R_\oplus}\right) - 1.019 \log_{10}\left(\frac{M_p}{M_\oplus}\right) \\ - 1.459 \log_{10}\left(\frac{R_\star}{R_\odot}\right) - 0.249 \log_{10}\left(\frac{a}{\mathrm{AU}}\right) \\ - 0.147\,(V - 5.0) + 0.193 \end{aligned} \tag{4}$$

for V the host star's apparent V-band magnitude (calibrated for $3 > V > 22$), R_p the planet radius, M_p the planet mass, $R_\star$ the star radius, and a the planet's semi-major axis. The coefficients are physically sensible: the 2.98 coefficient of R_p minus the 1.019 coefficient of M_p implies that the SNR depends inversely as bulk density, with puffier planets giving higher SNR for transit spectroscopy. Although this formula uses a V band magnitude ($\sim 0.5 - 0.6\mu$m), while NIRISS's SOSS mode covers $0.6 - 2.8\mu$m, the only difference using J band magnitudes is in the coefficients preceding the stellar radius and the semi-major axis terms (and thus implicitly, in the stellar mass). Focusing our analysis to a SNR measured by *JWST* is sensible given *TESS*'s role as a '*JWST* finder scope' [Deming et al., 2009]. We focus specifically on NIRISS given that it will likely be the workhorse *JWST* instrument for transmission spectroscopy [Beichman et al., 2014].

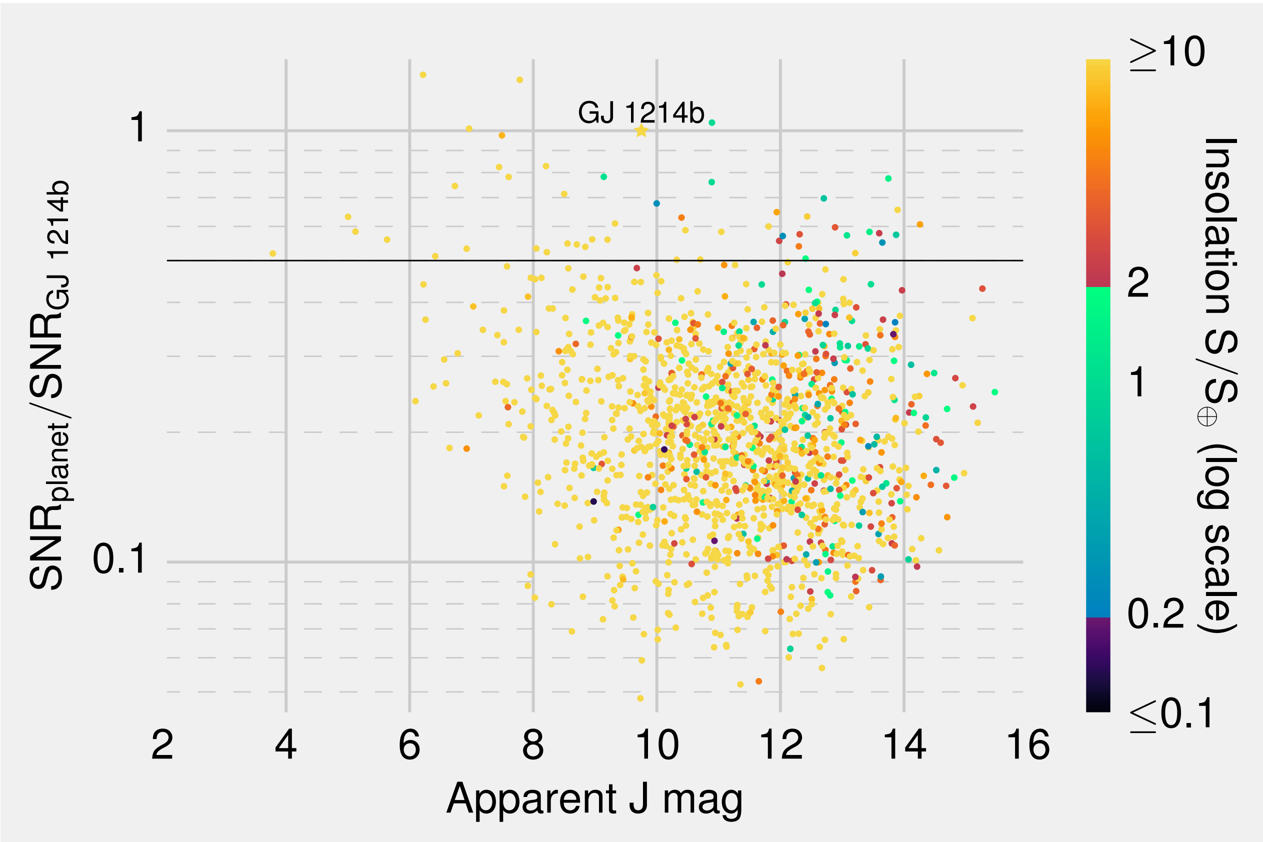

Figure 21: Scatter plot showing the SNR in transmission of detected planets with $R_p < 4R_\oplus$ from one Monte Carlo realization of all 3 years of the `HEMI` scenario. The SNR is computed from Eq. 4. Planets above the horizontal black line ($\mathrm{SNR_{planet}/SNR_{GJ\ 1214b}} = 0.5$) are counted for Fig. 15's metric of planets with 'good' atmospheres for transmission spectroscopy. GJ 1214b is marked with a star. The coloring of planets indicates their relative insolation, as well as whether they fall our ad-hoc habitable zone ($0.2 < S/S_\oplus < 2$).

Reference parameters for GJ 1214b are taken from Charbonneau et al. [2009]: $R_p = 2.678R_\oplus$, $M_p = 6.55M_\oplus$, $R_\star = 0.211R_\odot$, $a = 0.0144\mathrm{AU}$, $V = 15.1$. Using Eq. 4, we compute the SNR in transmission for all detected planets, for all extended mission scenarios. Fig. 21 shows one realization of the resulting distribution for planets detected in all three years of the `HEMI` scenario.

TESS mostly detects strongly irradiated planets (most points on Fig. 21 are yellow). A very small number, $\lesssim 10$, are both in the approximate habitable zone and also 'favorable for atmospheric characterization'. Of course, a highly compelling target with lower SNR in transmission per transit might merit a more ambitious *JWST* observing program. We note that all of these planets are assumed to have identical mean molecular weights and cloud properties.

More importantly, Fig. 15 shows that most of the planets with atmospheres that are best for transmission spectroscopy are already discovered after two years. The best extended missions (`HEMI+ECL`, `ECL-LONG`, `ECL-SHORT` and `ALLSKY`) boost the yield of such planets from ~ 100 to ~ 125. The worst, `POLE`, finds roughly 10. This best-case boost of $1.25\times$ more 'good' planets for atmospheric characterization is less than the relative boost of $1.6\times$ more newly detected long period planets. This latter point simply means that if we were to assign equal weights to both relative metrics, then $N_{\mathrm{new,atm}}$ would impact the decision of which extended mission to perform less than $N_{\mathrm{new,P<20d}}$.

6. $N_{\mathrm{new,new\ stars}}$: The observing strategy that collects the most photons from new stars should detect the most new planets about new stars. The `ECL-LONG` scenario dedicates 7 of a single year's 13 observing sectors to the ecliptic (where the other 5 are spent centered at the North Ecliptic Pole due to excessive Earth/Moon crossings). It consequently detects twice as many new planets about newly observed stars as the next-best scenarios: `ECL-SHORT` and `HEMI+ECL` (366 vs 171 and 161, respectively). These latter two options also spend time observing the ecliptic, but with only one camera, rather than with all four cameras simultaneously. We note that even though `ECL-LONG` is the scenario most successful in to detecting planets about new stars, only $\sim 30\%$ of its newly detected planets are actually from 'never-observed' hosts. [13]

[13] Dubbing these planets and hosts 'never-observed' neglects the question of overlapping fields with K2's observations (see discussion in Sec. 5)

7. $N_{\mathrm{new,SNR}\vee \mathrm{N_{tra}}}$: This statistic is the number of newly detected planets that are detected either (a) due to their final SNR clearing our threshold (logical) or (b) their number of observed transits being greater than or equal to 2. It is the complement to $N_{\mathrm{new,new\ stars}}$: scenarios like `HEMI`, `POLE`, and `ALLSKY` that do not observe many new stars will detect all of their planets from a boosted SNR and/or clearing the minimum transit threshold.

Comment on meaning of 'detected in postage stamps' vs 'detected in FFIs'
The invested reader may inquire "what about the cross-over case of planets that are observed as PSs during the primary (extended) mission, but as FFIs in the extended (primary) mission? These are not explicitly listed in Fig. 15". When describing the entire unique planet population detected from Years 1-3, for simplicity of language we use 'postage stamp detections' to refer to planets that are observed at any time (primary or extended missions) at 2 minute cadence. In these cases, the dominant contribution to the final signal to noise ratio tends to come from the PS observations. When describing new planet detections, we use 'postage stamp detections' to mean planets

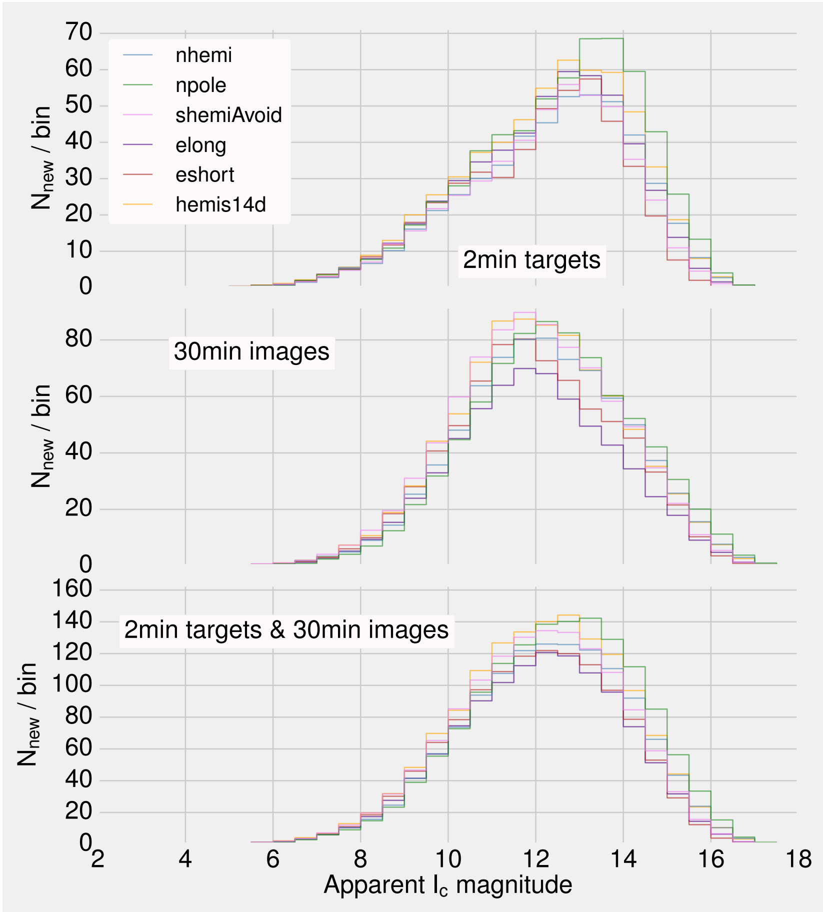

Figure 22: Histogram of apparent I_c magnitude of host star for newly detected $R_p < 4R_\oplus$ planets from all extended mission scenarios, for *top:* postage stamp detections, *middle:* full frame image detections, *bottom:* the sums thereof. While `POLE` does well by most metrics, a larger proportion of the new planets it detects orbit dim stars compared to alternatives like `ALLSKY` or `HEMI+ECL`.

that were newly detected due to being observed as postage stamps in the extended mission. In other words, this 'cross-over' point only matters in discussions of the unique planet population from an entire mission, Years 1-3. Considering just the newly detected planet population, we can unambiguously specify whether the new detections came from full frame images or postage stamps, irrespective of their observations from the primary mission.

4.4 *On the brightness of stars with detected planets*

While `POLE` does well by most metrics, a larger proportion of its newly detected planets orbit dim stars than the planet populations detected from alternatives like `ALLSKY` or `HEMI+ECL`. We demonstrate this in Fig. 22. The main point here is that if in mission selection we were to assign extra weight towards detecting planets orbiting bright host stars, then `POLE` would do the worst. For instance, arbitrarily setting the bound at $I_c < 10$ and numerically integrating from Fig. 22's

HEMI	POLE	HEMI+ECL	ECL-LONG	ECL-SHORT	ALLSKY
162	154	190	167	183	198

Table 2: Number of new, $I_c < 10$, $R_p < 4R_\oplus$ planets from each extended mission (average of 50 Monte Carlo realizations of our code; showing sum of PSs & FFIs). `POLE` detects the fewest new planets orbiting bright stars.

data, we see in Table. 2 that there is a $\sim 30\%$ level difference between the missions. For point of reference, the primary mission detects 386 such planets – so a single year of extended mission detects roughly as many planets orbiting bright hosts as a single year of primary mission.

5 Discussion

5.1 What's best on a > 1 year horizon for planet detections?

TESS's orbit is stable, in principle, for more than 1000 years [Gangestad et al., 2013]. While minor mechanical failures should be expected on the timescale of a few years, it is plausible that the spacecraft could outlive both the 2-year primary mission and the 1-year extended mission. Therefore, when choosing any particular plan for a 1-year Extended Mission, it makes sense to also consider the implications of an even longer Extended Mission.

A simple point is that `HEMI`, `POLE`, and `HEMI+ECL` can all be inverted to their southern or northern complements for a fourth year of observing. This will yield a comparable number of new planets to what they find in year 3 ($\mathcal{O}(1300)$ with $R_p < 4R_\oplus$). This argues strongly to continue observing the entire sky, rather than focusing on a single ecliptic hemisphere after the primary mission's completion. This would continue *TESS*'s role as a planet-discovery machine, while also addressing the practical matter of refining ephemerides in order to enable detailed characterization with suitable instruments.

The `ECL-LONG`, `ECL-SHORT`, and `ALLSKY` scenarios are less obviously extensible to multiple years. The main reasons to return to the ecliptic after performing `ECL-LONG` or `ECL-SHORT` would be to make *TESS*'s survey truly 'all-sky', and to complete all possible *K2* follow-up observations (see discussion below). Of course, this would need to happen during intervals in which the Moon and Earth were not in the way.

Any of our proposed scenarios could simply be repeated indefinitely (as could their two-year 'all-sky' versions). This presents a trade-off that becomes apparent by comparing two particular two-year missions: (1) two years of `ALLSKY` (2) repeating the two-year Primary Mission. If we repeat the primary mission over 2 years, the northern and southern CVZs each get 1 year of continuous observation. If we execute `ALLSKY` for 2 years, the northern and southern 'long viewing zones' each get 2 years of 14-day windowed observations. The latter case allows 2-transit detections of $P \lesssim 1$ year planets over 2% of the sky. The former allows 2-transit detections of $P \lesssim 6$ month planets over 1% of the sky. This simple consideration of course misses that point that data obtained from repeating the primary mission would be less subject to aliasing problems and would have fewer period ambiguities. That said, repeating `ALLSKY` for two years might be a middle ground between the two extreme strategies "repeat `POLE` indefinitely" and "repeat the primary mission indefinitely".

A longer-term question is "when will *TESS* hit the point of diminishing returns?" The 'low-hanging fruit' of small planets transiting bright stars at short orbital periods will eventually be found if *TESS* continues to observe the same sky. The most important qualitative point of this memo, made in Fig. 16, is that after *TESS*'s primary mission there will be many objects remaining for which merely doubling the number of observed transits will enable their detection. Eventually though, the peak of the phase-folded SNR distribution shown in Fig. 16 will shift past the detection threshold, and more observations will only allow us to probe out to longer orbital periods and dimmer stars. No detailed study has yet quantified when *TESS* will reach this operating regime.

5.2 *The ephemeris problem*

Analytic motivation For follow-up observations, we will often need to predict future times of transits or occultations, ideally with an accuracy of an hour or less. After enough time has passed that the uncertainty has grown to a significant fraction of the orbital period, we say that the ephemeris has gone "stale", presenting a major obstacle to many follow-up programs. For *TESS*'s ground-based follow-up campaign, the problem of a stale ephemeris could double or triple the amount of observing time that is required for a successful result. Likewise, for planning space-based observations, for which observing time is always scarce, it is extremely important to have a reliable and accurate ephemeris. For mass determination through the Doppler method, a stale transit ephemeris adds uncertainty to the planetary mass measurements, by increasing the number of effectively free parameters.

Consider then the problem of estimating $\sigma_{t_c}(T_x)$, the uncertainty of the mid-transit time σ_{t_c} for a given planet at some time T_x following its last-observed transit. We begin analytically: assume that the planet has $N_{\rm tra} = 2$ observed transits, spaced an orbital period $P = 14$ days apart. Because that period is one half the nominal *TESS* dwell time of a given pointing, it represents the shortest period for which typically $N_{\text{tra}} = 2$, and as such the worst-case scenario for predicting the times of future transits, amongst cases with $N_{\text{tra}} > 1$. Given two mid-transit times, each measured with the time's uncertainty σ_0, separated by P, the uncertainty of a future mid-transit time can be derived by standard least-squares fitting and propagation of errors (*e.g.* Lyons [1991], Equation 2.18):

$$\sigma_{t_c}(T_x) = \sigma_0 \sqrt{1 + 2T_x/P + 2(T_x/P)^2} \tag{5}$$

Note that for observing future transits, $E \equiv T_x/P$ is an integer, and the above equation can be re-expressed:

$$\sigma_{t_c}(E) = \sigma_0 \sqrt{1 + 2E + 2E^2}, \tag{6}$$

which is bounded by the simpler approximation:

$$\sigma_{t_c}(E) \lesssim \sigma_0 \left(1 + \sqrt{2}E\right), \tag{7}$$

which is exact at $E = 0$, has a maximum 8% fractional error at $E = 1$, and becomes increasingly accurate as E increases. By $E = 20$, the fractional error of the latter approximation is less than 1%.

For $T_x = 2$ years and $P = 2$ weeks, then $E \approx 50$, so $\sigma_{t_c} \approx 75\sigma_0$. At 2-minute cadence, a typical value for the per-transit timing uncertainty is $\sigma_0 = 4$ minutes, and the predicted uncertainty on its mid-transit time is 5 hours two years later or 10 hours four years later. This leads to a simple rule of thumb:

> For a two-transit super-Earth, the uncertainty in the predicted transit time, in hours, is numerically equal to about $2Y$, where Y is the number of years after the Primary Mission.

If the transits are observed only at 30-minute cadence, then uncertainty will be roughly 4 times greater: $\sigma_0 \sim 16$ minutes. This claim ("4× greater") is based on Figure 9 of [Price and Rogers, 2014], a plot of the effects of finite cadence on timing precision. We compared the precisions of 2-min and 30-min cadences for their specific example of $P = 10$ days and a dwell time of 1 month.

On the other hand, Fig. 18 shows that 7 in 8 of the planets detected by *TESS*'s main mission will have $N_{\text{tra}} > 3$ and so their ephemerides should be better than the example derived analytically above. Rather than generalize the analytic equations, we resort to numerical simulations in order to predict the uncertainties of mid-transit times for planets expected to be discovered by *TESS*'s main mission.

Numerical analysis We start with the analytic form Price and Rogers [2014] derive for the per-transit uncertainty on the mid-transit time σ_0:

$$\sigma_0 = \frac{1}{Q}\sqrt{\frac{\tau T}{2}}\left(1 - \frac{t}{3\tau}\right)^{-1/2}$$

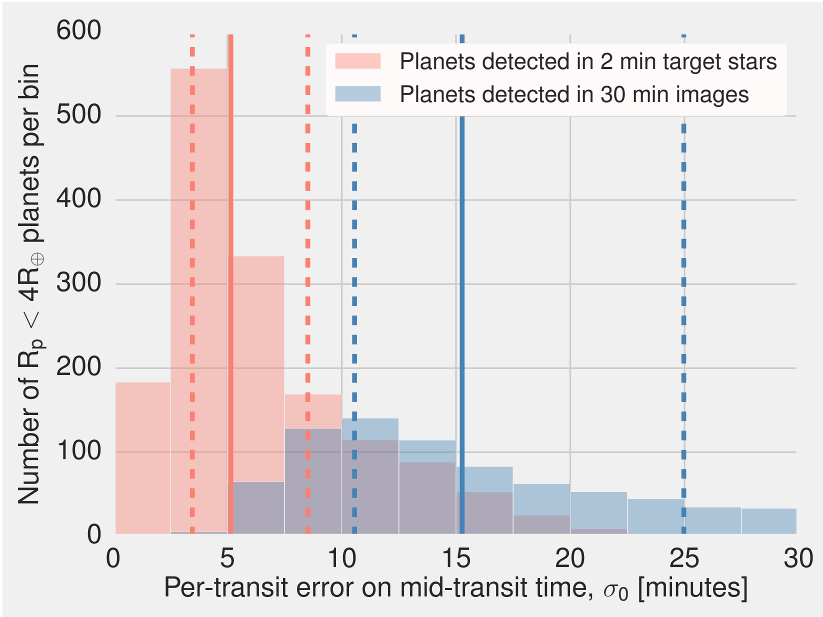

Figure 23: Uncertainty of mid-transit time on a single transit, σ_{t_c}, for all detected $R_p < 4R_\oplus$ planets from the primary mission as computed from Eq. 8. Solid lines are medians, dashed lines are 25th and 75th percentiles.

when $\tau \geq t$ and

$$\sigma_0 = \frac{1}{Q}\sqrt{\frac{tT}{2}}\left(1 - \frac{\tau}{3t}\right)^{-1/2} \tag{8}$$

when $t > \tau$, where Q is the SNR per transit, t is the cadence, T is the transit duration, and τ is the ingress (or egress) time. We have all the later terms from our yield simulation, and show the resulting distribution of σ_0 in Fig. 23. Indeed, our suggested σ_0 of about 4 minutes for postage stamps and 16 minutes for full frame images is reasonable, which is good because we computed the former from the $t \to 0$ limit of Eq. 8 originally derived by Carter et al. [2008].

Given the distributions on per-transit uncertainty of t_c, we then took an example planet with 4 transits. We drew "observed" mid-transit times from a Gaussian with zero mean and standard deviation σ_0, and then ran a linear least squares regression. We then added just one data point 1 year after the final observed transit, and repeated the regression. This produces a cartoon-plot, Fig. 24, which confirms two expected points:

1. Years after the initial discovery, the uncertainty of mid-transit time is of order hours.

2. If we detect an additional transit 1 year after the final observed transit from the primary mission, the uncertainty on the mid-transit time decreases by an order of magnitude.

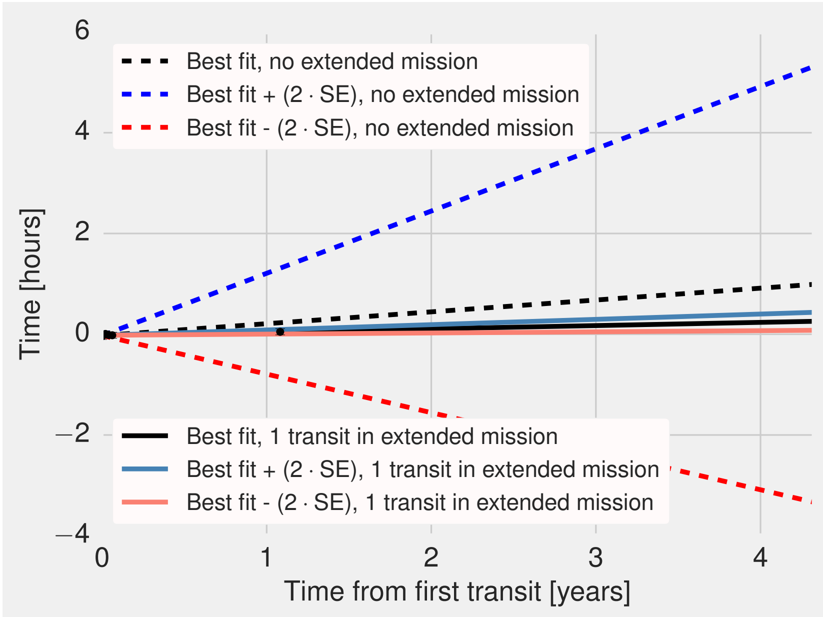

Figure 24: Observed mid-transit times (dots) and best fits to a linear ephemeris (lines). The dotted lines fit 4 data points from a nominal planet. 'SE' is the standard error on the slope which multiplied by 1.96 (rounded to 2 in the legend) gives a 95% confidence interval by subtracting blue and orange lines.

We proceed by repeating the above procedure for every planet, and evaluate typical 95% confidence intervals ("uncertainties", loosely) for t_c, at typical times after the first transits, for all of our detected planets. Specifically, we take them at $T_x = 2$ and 4 years, and get Fig. 25. This figure confirms (top left panel) our analytic expectation that the uncertainty of mid-transit times in hours should be somewhat less than twice the number of years after *TESS* first observes the planet at 2-min cadence, since most such planets have $N_{\rm tra} \geq 4$. It also confirms our rough expectation that the uncertainty on FFI mid-transit times is roughly 4 times that of postage stamps, although the uncertainties on FFIs have a much more uniform tail.

More importantly, Fig. 25 emphasizes the importance of refining *TESS*'s ephemerides: if we do not, the typical *TESS* planet will have many hours of uncertainty on its mid-transit time a few years following its detection. If we do follow-up, we will know when the planet transits to $\lesssim 1$ hour for many more years. This argues strongly for an extended mission which, whether over 1 or 2 years, re-observes many if not all of the targets that *TESS* detects in its primary mission. The smallest-radius Earths and super-Earths may otherwise be much more difficult to follow up, due to a stale ephemeris.

5.3 *Risks and caveats*

Risk that planet detection simulation gets yield wrong: What is the risk that we over or under-estimated *TESS*'s planet yield, either in the

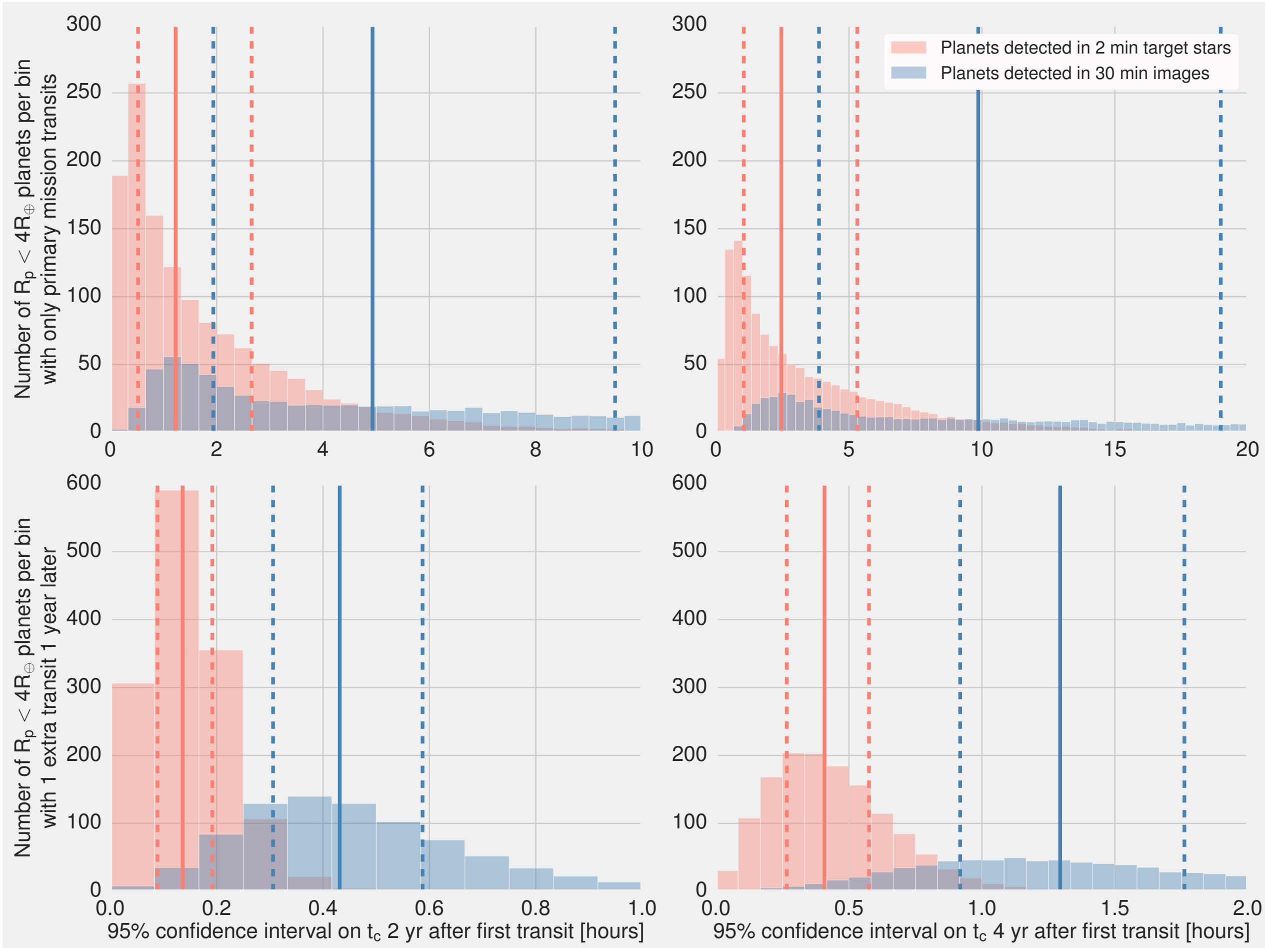

Figure 25: *Top row*: histogram of 95% confidence intervals 2 (*left*) and 4 (*right*) years following the first detected transit in the primary mission. 20 minute bins. *Bottom row*: histogram of 95% confidence intervals 2 (*left*) and 4 (*right*) years following the first detected transit in the primary mission, but with an additional data point added to the analog of Fig. 24 one year after the transit in the initial time series (5 minute bins). Note that the top row's timescale is an order of magnitude more than the bottom row. Solid lines are medians, dashed lines are 25$^{\text{th}}$ and 75$^{\text{th}}$ percentiles.

primary mission, or in any given extended mission? We summarized the assumptions that went into our yield calculations in Sec. 3.7. We made them believing that they were all good enough for useful relative comparisons of different sky-scanning scenarios, even if they are not correct in absolute terms to better than ∼50%.

Highlighting a few of these assumptions, in order of what we feel is decreasing concern:

1.) We assume no knowledge of the outcomes of prior transit searches. As indicated in the text, this assumption is worst for the `ECL-LONG` and `ECL-SHORT` scenarios, for which *K2* and *TESS*'s overlap will be important. Estimating the magnitude of our error, assume *K2* will have observed 70% of the sky in the $|\beta| < 6°$ band about the ecliptic by 2019. Of the 1169 'new' $R_p < 4R_\oplus$ planets that *TESS* detects in `ECL-LONG`, 502 of them are within $|\beta| < 12°$ of the ecliptic. Assuming that all of these detections are uniformly distributed over the $|\beta| < 12°$ band, this means that 35% (the ratio of the annuli) of *TESS*'s new planets will already have been detected in *K2* data. This simple estimate quantifies our global error in reporting 'new' planets near the ecliptic, but avoids the issue of merging the two datasets to discover long period planets. This latter opportunity could be an important reason to actually do `ECL-LONG` or `ECL-SHORT` and thus demands detailed study, which we recommend below.

2.) The difference in $1.25R_\oplus < R_p < 2R_\oplus$ planet yield from S+15. We discussed this point in Sec. 4.1. S+15 claim that *TESS* detects roughly 900 super-Earths in full frame images, and 500 in postage stamps. We claim that *TESS* detects roughly 10 super-Earths in full frame images, and 400 in postage stamps. This is a discrepancy of a factor of 4 in one of *TESS*'s most significant data products.

We do not understand the origin of the difference between our method and S+15's. That said, based on *(a)* raw output data generated by the author of S+15 and dated in May 2015 (3 months after initial ApJ submission, 1 month before acceptance); *(b)* the data we generated from the earliest available version of S+15's code, dated in October 2015 (before any of our methodological changes); *(c)* the analytic estimates of Winn [2013] which predict ~ 300 super-Earth detections; and *(d)* a plausibility argument presented in Sec. 4.1 that showed S+15's results implied a detection efficiency biased sub-linearly in R_p, whilst ours implies a bias between linear and quadratic in R_p, we think that the current simulations give a more accurate picture.

3.) We use a SNR threshold of 7.3. This number was computed by S+15 based on the argument that it would be a sufficient threshold to give one false positive per 2×10^5 light curves. This criterion is a self-consistent ad-hoc choice that we made for target stars. Applying the same criterion to full frame images would lead to more than one false positive, since full frame images come from a much larger sample of stars. Any pipeline that is written to work with *TESS* data will confront this problem: processing 10^8 vs. 4×10^6 vs. 2×10^5 stars requires different false positive thresholds. Extrapolating from S+15's Fig 15, a threshold sufficient to give 0.05 false positives per 2×10^5 light curves, or 1 false positive per 4×10^6 light curves (as from our full frame images), is roughly 7.5. Making the same ad-hoc estimate that S+15 did and multiplying by 1.03 for the expected drop in SNR from cosmic ray noise gives a SNR threshold of 7.7 for full frame images. Considering our Fig. 16 (and noting the black line is for the sum of postage stamp and full frame image detections), adopting a SNR threshold of 7.7 for FFIs would mean a loss of $\sim 30 \times 4 = 120$ planets over two years, or 60 of what we claim are 'detected planets' from full frame images in 1 year's extended mission.

4.) We use synthetic stars from a single galactic model (TRILEGAL). One check on the robustness of this model would be to compare with other galactic models like GALAXIA [Sharma et al., 2011] or a Besaçon model [Robin et al., 2003]. We have already done this using a simple analytic model by Winn [2013], which agrees with our work to factors of a few. We might eventually use the real star catalog that *TESS*'s Target Selection Working Group is assembling, but this would come with large uncertainties on stellar radii, effective temperatures, and companion fractions.

While we recommend that these broader checks be performed in future *TESS* yield calculations, they are excessive for the purposes of this report given that we only used the nearest, brightest, stars ($d \lesssim 1$kpc, $I_c \lesssim 16$) with a simple prescription for background contamination in evaluating *TESS*'s $R_p < 4R_\oplus$ detections. The relative uncertainties become much greater if we try to estimate detections of giant planets and false positives throughout the galactic disk. That said, we take S+15's cross-checks (cf Fig. 5 of that paper) against actual surveys of the local stellar population as indicative that we probably have the number of nearby stars, as well as their properties, correct to our desired factor of 2.

5.) At least 2 transits for detection: recall Figs. 17 and 18. If we were to use a more stringent criteria, for instance at least 3 transits for detection as the *Kepler* pipeline currently does, we would lose $\mathcal{O}(200)$ of the planets detected in the primary mission, and $\mathcal{O}(100)$ from the extended missions. This assumption disproportionately affects long-period planets.

6.) We neglect instrument aging, spacecraft systematics, etc. To our best knowledge detailed models do not currently exist for how *TESS*'s optics and CCDs will degrade with time. We are also assuming that, as with *K2* , time-correlated spacecraft level systematics can be removed in post-processing. These assumptions are reasonable at our current state of pre-flight knowledge, and will need to be changed accordingly as the mission progresses. If we were to assume a gradual decline in photometric performance, for instance from an increased number of dead or 'hot' pixels, the relative extended-mission-to-extended-mission comparisons would remain identical. The absolute extended-mission-to-primary-mission yields would decrease.

7.) We do not consider the efficacy of processing pipeline. For instance, `ALLSKY` will come with period ambiguities and aliasing problems imposed by its 14 day sampling at the 'continuous' viewing zones. Similar issues are generic across extended missions for which we detect a small number of transits in the primary mission, and then a small number of transits in the extended mission.

A robust way to approach this problem would be to generate a synthetic simulated *TESS* dataset, *i.e.*, at the image-level, rather than at the idealized phase-folded SNR level from this work, for each extended mission's observations. Then actually perform astrometry on injected stars, extract light curves, de-trend them, and find their transits. This exercise would likely also be a useful way to prepare the SPOC and broader community for what we expect the era of *TESS* photometry to entail in terms of data quality.

Miscellaneous risks To be considered as knowledge of *TESS*'s inflight performance improves:

- What is the risk of not meeting 'threshold' science – essentially whatever goals the science team decides will be the main drivers for an extended mission?
- Is there a risk of excessive false positives, for instance from field crowding, from any particular extended mission? This is primarily an issue for fields near the galactic plane and bulge.
- Would any expected partial instrument failures make a certain observing scenario infeasible? (à la *K2*, for instance)

6 Concluding remarks and recommendations

This trade-study laid out technical requirements, science goals, opportunities, and risks relevant towards observing with *TESS* after its first two years. The baseline science requirements for *TESS*'s primary mission are defined [Ricker et al., 2014], and an extended mission offers a chance to re-prioritize. Is securing *TESS*'s ephemerides more important than probing out to the longest period planets? Are the variations in absolute new planet yields, at $\lesssim 30\%$ between all the extended missions, more valuable than other desires and opportunities?

6.1 Recommendations

Analyze target prioritization problem and decide whether or not to optimize target selection based on results. Planet occurrence rates are functionally dependent on a star's properties – should this affect which stars we give upgraded cadence? Is our proposed `Merit` statistic (Eq. 2) how we want to prioritize targets?

Optimize cadence: 200k at 2min vs. 400k at 4min, & related trade-offs. Ideally a metric would be devised that quantifies, for each star, how much *improvement* would result from observing at short-cadence versus long-cadence, and only those stars for which short-cadence would deliver the *most significant benefit* would be selected. We suspect that the number of short-cadence stars could be greatly reduced, with little effect on the planet detection statistics. This would allow the FFIs to be returned at a higher cadence, which would likely be desirable.

Take steps to address the 'upgrading cadence' problem: if there is a likely transiting planet in full frame image data, upgrading the planet to short cadence in future observing sectors improves the probability and fidelity of detection.

Guest Investigator Office / TESS Science Office: solicit advice from experts in asteroseismology and variable-sky astronomy to understand how extended missions affect their science cases (*e.g.*, data throughput rates are particularly important for time-sensitive supernovae observations). More broadly, solicit community feedback during the process of defining the extended mission. This may entail a call for white papers, comments on this report, or direct proposals to the GI office. As exemplified in NASA's 2016 Astrophysics Senior Review, everyone benefits from the discussions generated by such community feedback [Donahue et al., 2016].

Decide (explicitly or implicitly) on weights between our proposed metrics. Perhaps also brainstorm others – Sec. 3.3 gives a summarized list. Are the $\lesssim 30\%$ variations in absolute new planet yields more valuable than other desires or opportunities?

Simulate combining TESS and K2 data from `ECL-LONG` *and* `ECL-SHORT`. This is perhaps the most important qualitative difference between observing towards and away from the ecliptic. Would *TESS*+*K2* enable more discoveries out at long periods than alternatives? How many of the new planets that *TESS* detects on the ecliptic will actually be detected by *K2* ? Is the value-added of combining datasets a compelling case compared with discovery?

Further topics for study: 1.) After how many years would the planet yield start to show steeply diminishing returns? Suppose, for example, the Primary Mission were repeated indefinitely. How much dimmer would the host stars of new planets be, in each year? in such a scenario? Would the planets tend to be smaller? Would there be fewer of them? *2.)* Study the limiting case of `ALLSKY` for 2 years, vs primary mission repeat for 2 years, vs `POLE`$\times$2 for 2 years. The most interesting aspect here is the continuous viewing zones: 2 CVZs at 14-day sampling, vs. 2 CVZs at continuous sampling for one-year each, vs. 1 CVZ for full sampling over two years.[14]

[14] Our simplified perfect period extraction would miss challenges from the data processing.

Acknowledgements

We thank Peter Sullivan for his support in the early phases of this work and for his helpful comments on our results. We also are grateful to Jack Lissauer for input regarding the value of observing *Kepler*'s field with *TESS*. The *TESS* project provided the computing resources used in this work and Ed Morgan, Isaac Meister, and Kenton Philips provided the support to keep the machines running.

Facility: *TESS*

Software: matplotlib [Hunter, 2007], NumPy [Walt et al., 2011], SciPy [Jones et al., 2001], pandas [McKinney], JPL NAIF's SPICE library [Acton, 1996], and the IDL Astronomy User's Library [Landsman, 1995].

Resources: This research has made use of the NASA Astrophysics Data System and the NASA Exoplanet Archive. The NASA Exoplanet Archive is operated by the California Institute of Technology, under contract with the National Aeronautics and Space Administration under the Exoplanet Exploration Program. This paper also makes use of data collected by the Kepler mission. Funding for the Kepler mission is provided by the NASA Science Mission directorate.

Appendices

A Models relevant to Earth-Moon crossings

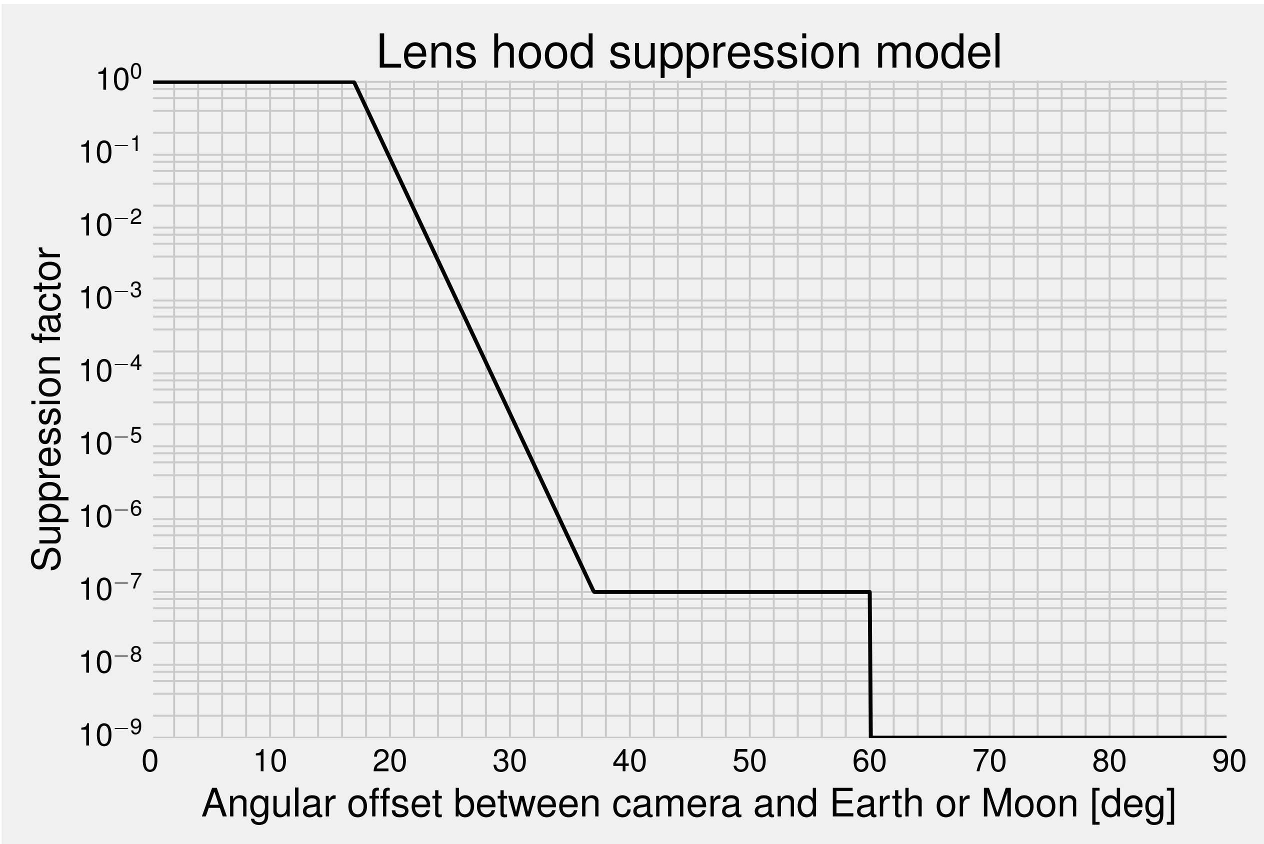

Figure 26: Lens hood suppression plotted against the angular offset to the Earth or Moon. This suppression factor is defined as the fraction of incident flux that is blocked by the spacecraft, sunshade, lens hood, or combinations thereof.

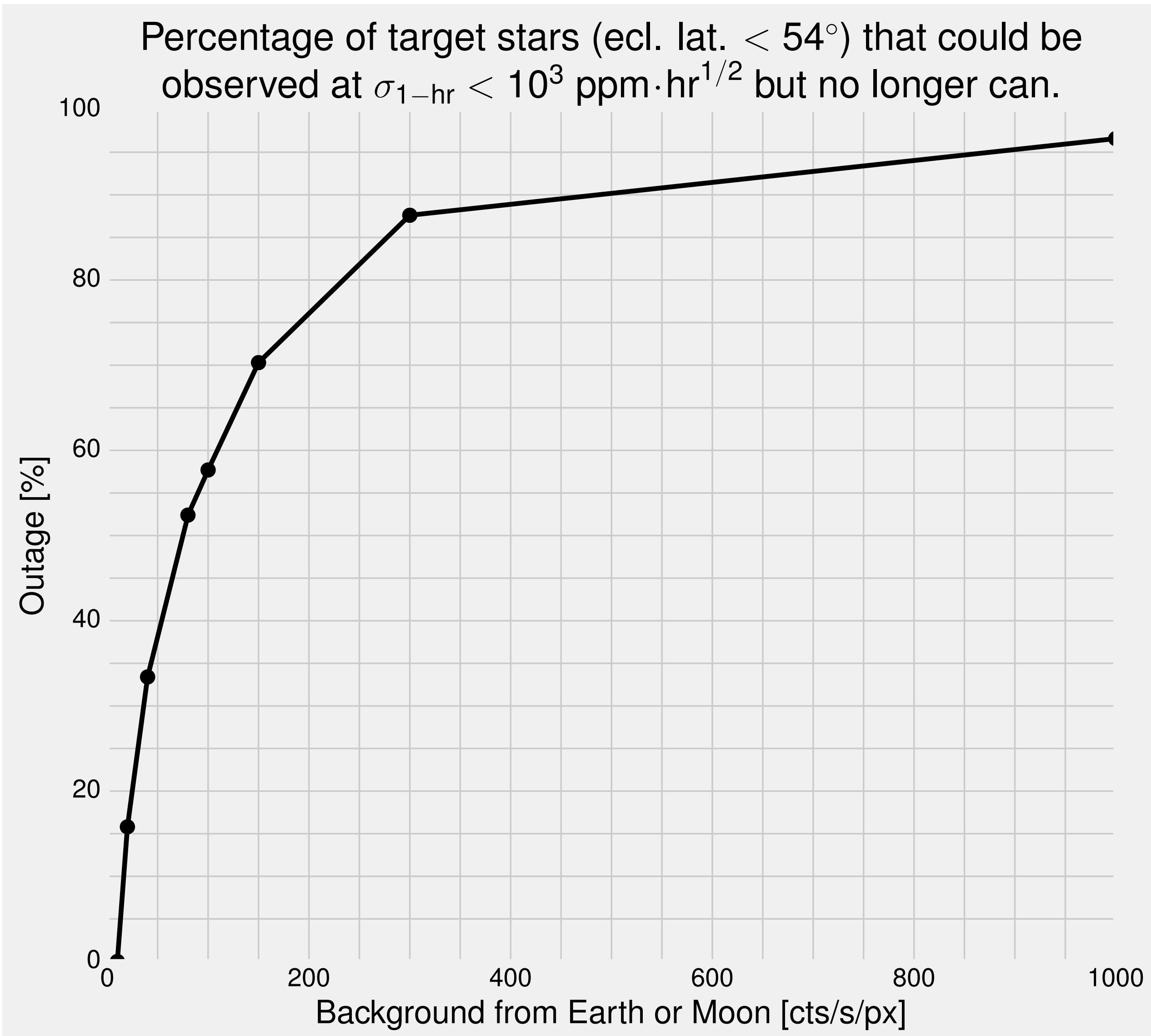

Figure 27: The procedure described in Sec. 3.6 drops fields in which ∼90% of the target stars (in the lower two camera fields) cannot be observed.

B Changes from Sullivan et al. [2015]

On the angular dependence of TESS's pixel response function: In our SNR calculation, we do not keep track of individual times for every transit. How then do we assign PSFs to different transits from the same object that fall on different regions of the CCDs, and thus should have slightly better or degraded PSFs? (Largest cumulative flux fraction at the CCD's center, smallest at the corners).

S+15 dealt with this by computing the mean of all the field angles (distance from the center of the CCD axis), and then passing this mean into a look-up table for PSFs based on four PSFs that had been computed from a ray-tracing model at four different field angles. S+15 then 'observes' each eclipsing object with a single class of PSF. This leads to the implausible phenomenon that extra observations can actually *lower* the SNR of an eclipsing object if they are taken with an unfavorable field angle/PSF. This effect is largely off-set by the extra pointing increasing the SNR, but for extended missions (coming back to the same objects at potentially very different field angles) it winds up reducing observed SNR for $\sim$3% of detected objects.

In extended missions (as well as in the primary mission) we expect stars to land on very different regions of the CCD over the course of being observed. We simplify this in our work by assuming that all stars land on the center of the *TESS* CCDs (the green curve of S+15 Fig. 13). This assumption is justified because our chief point of quantitative comparison is the ability of different pointing strategies to impact *TESS*'s planet yield in extended missions, and there is little *a priori* reason to assume that any one pointing scenario should be biased for an extra amount of stars to land on the 'bad regions' of *TESS*'s CCDs.

References

C. H. Acton. Planetary data system: Ancillary data services of NASA's Navigation and Ancillary Information Facility. *Planetary and Space Science*, 44(1):65–70, Jan. 1996. ISSN 0032-0633. doi: 10.1016/0032-0633(95)00107-7. URL http://www.sciencedirect.com/science/article/pii/0032063395001077.

I. Baraffe and G. Chabrier. Mass–Spectral Class Relationship for M Dwarfs. *The Astrophysical Journal*, 461(1), Apr. 1996. ISSN 0004637X. doi: 10.1086/309988. URL http://stacks.iop.org/1538-4357/461/i=1/a=L51.

G. Basri, L. M. Walkowicz, and A. Reiners. Comparison of Kepler Photometric Variability with the Sun on Different Timescales. *The Astrophysical Journal*, 769(1):37, 2013. ISSN 0004-637X. doi: 10.1088/0004-637X/769/1/37. URL http://stacks.iop.org/0004-637X/769/i=1/a=37.

C. Beichman, B. Benneke, H. Knutson, R. Smith, P.-O. Lagage, C. Dressing, D. Latham, J. Lunine, S. Birkmann, P. Ferruit, G. Giardino, E. Kempton, S. Carey, J. Krick, P. D. Deroo, A. Mandell, M. E. Ressler, A. Shporer, M. Swain, G. Vasisht, G. Ricker, J. Bouwman, I. Crossfield, T. Greene, S. Howell, J. Christiansen, D. Ciardi, M. Clampin, M. Greenhouse, A. Sozzetti, P. Goudfrooij, D. Hines, T. Keyes, J. Lee, P. McCullough, M. Robberto, J. Stansberry, J. Valenti, M. Rieke, G. Rieke, J. Fortney, J. Bean, L. Kreidberg, D. Ehrenreich, D. Deming, L. Albert, R. Doyon, and D. Sing. Observations of Transiting Exoplanets with the James Webb Space Telescope (JWST). *Publications of the Astronomical Society of the Pacific*, 126:1134–1173, Dec. 2014. doi: 10.1086/679566.

Z. Berta-Thompson, I. Ribas, S. Seager, and L. Bouma. Projects for a TESS and CHEOPS Collaboration. TESS Internal Report, MIT, June 2016.

C. J. Burke, S. T. Bryson, F. Mullally, J. F. Rowe, J. L. Christiansen, S. E. Thompson, J. L. Coughlin, M. R. Haas, N. M. Batalha, D. A. Caldwell, J. M. Jenkins, M. Still, T. Barclay, W. J. Borucki, W. J. Chaplin, D. R. Ciardi, B. D. Clarke, W. D. Cochran, B.-O. Demory, G. A. Esquerdo, I. Thomas N. Gautier, R. L. Gilliland, F. R. Girouard, M. Havel, C. E. Henze, S. B. Howell, D. Huber, D. W. Latham, J. Li, R. C. Morehead, T. D. Morton, J. Pepper, E. Quintana, Darin Ragozzine, S. E. Seader, Y. Shah, A. Shporer, P. Tenenbaum, J. D. Twicken, and A. Wolfgang. Planetary Candidates Observed by Kepler IV: Planet Sample from Q1-Q8 (22

Months). *The Astrophysical Journal Supplement Series*, 210(2):19, 2014. ISSN 0067-0049. doi: 10.1088/0067-0049/210/2/19. URL http://stacks.iop.org/0067-0049/210/i=2/a=19.

J. A. Carter, J. C. Yee, J. Eastman, B. S. Gaudi, and J. N. Winn. Analytic approximations for transit light-curve observables, uncertainties, and covariances. *The Astrophysical Journal*, 689(1):499, 2008. URL http://iopscience.iop.org/0004-637X/689/1/499.

D. Charbonneau, Z. K. Berta, J. Irwin, C. J. Burke, P. Nutzman, L. A. Buchhave, C. Lovis, X. Bonfils, D. W. Latham, S. Udry, R. A. Murray-Clay, M. J. Holman, E. E. Falco, J. N. Winn, D. Queloz, F. Pepe, M. Mayor, X. Delfosse, and T. Forveille. A super-Earth transiting a nearby low-mass star. *Nature*, 462(7275):891–894, Dec. 2009. ISSN 0028-0836, 1476-4687. doi: 10.1038/nature08679.

D. Deming, S. Seager, J. Winn, E. Miller-Ricci, M. Clampin, D. Lindler, T. Greene, D. Charbonneau, G. Laughlin, G. Ricker, D. Latham, and K. Ennico. Discovery and Characterization of Transiting Super Earths Using an All-Sky Transit Survey and Follow-up by the James Webb Space Telescope. *Publications of the Astronomical Society of the Pacific*, 121(883):952, 2009. ISSN 1538-3873. doi: 10.1086/605913. URL http://stacks.iop.org/1538-3873/121/i=883/a=952.

M. Donahue, M. Bautz, R. Green, G. Hasinger, L. Kaltenegger, H. Krawczynski, A. MacFayden, D. McCammon, R. Oppenheimer, P. Szkody, and D. Zaritsky. 2016 NASA Astrophysics Senior Review. Technical report, NASA, Feb. 2016. URL http://science.nasa.gov/media/medialibrary/2016/06/09/Main_Panel_SR2016_Report_FinalTAGGED.pdf.

C. D. Dressing and D. Charbonneau. The Occurrence of Potentially Habitable Planets Orbiting M Dwarfs Estimated from the Full Kepler Dataset and an Empirical Measurement of the Detection Sensitivity. *arXiv preprint arXiv:1501.01623*, 2015. URL http://arxiv.org/abs/1501.01623.

D. A. Fischer and J. Valenti. The Planet-Metallicity Correlation. *The Astrophysical Journal*, 622:1102–1117, Apr. 2005. ISSN 0004-637X. doi: 10.1086/428383. URL http://adsabs.harvard.edu/abs/2005ApJ...622.1102F.

F. Fressin, G. Torres, D. Charbonneau, S. T. Bryson, J. Christiansen, C. D. Dressing, J. M. Jenkins, L. M. Walkowicz, and N. M. Batalha. THE FALSE POSITIVE RATE OF *KEPLER* AND THE OCCURRENCE OF PLANETS. *The Astrophysical Journal*, 766(2):

81, Apr. 2013. ISSN 0004-637X, 1538-4357. DOI: 10.1088/0004-637X/766/2/81.

J. W. Gangestad, G. A. Henning, R. R. Persinger, and G. R. Ricker. A high Earth, lunar resonant orbit for lower cost space science missions. *arXiv preprint arXiv:1306.5333*, 2013. URL http://arxiv.org/abs/1306.5333.

L. Girardi, M. A. T. Groenewegen, E. Hatziminaoglou, and L. da Costa. Star counts in the Galaxy: Simulating from very deep to very shallow photometric surveys with the TRILEGAL code. *Astronomy and Astrophysics*, 436(3):895–915, June 2005. ISSN 0004-6361, 1432-0756. DOI: 10.1051/0004-6361:20042352. URL http://www.edpsciences.org/10.1051/0004-6361:20042352.

G. M. H. J. Habets and J. R. W. Heintze. Empirical bolometric corrections for the main-sequence. *Astronomy and Astrophysics Supplement Series*, 46:193–237, Nov. 1981. ISSN 0365-0138.

T. J. Henry, W.-C. Jao, J. P. Subasavage, T. D. Beaulieu, P. A. Ianna, E. Costa, and R. A. Méndez. The solar neighborhood. XVII. Parallax results from the CTIOPI 0.9 m program: 20 new members of the RECONS 10 parsec sample. *The Astronomical Journal*, 132(6):2360, 2006. URL http://iopscience.iop.org/1538-3881/132/6/2360/205485.web.ps.gz.

J. D. Hunter. Matplotlib: A 2d Graphics Environment. *Computing in Science & Engineering*, 9(3):90–95, 2007. ISSN 1521-9615. DOI: 10.1109/MCSE.2007.55. URL http://ieeexplore.ieee.org/lpdocs/epic03/wrapper.htm?arnumber=4160265.

J. A. Johnson, K. M. Aller, A. W. Howard, and J. R. Crepp. Giant Planet Occurrence in the Stellar Mass-Metallicity Plane. *Publications of the Astronomical Society of the Pacific*, 122(894):905, 2010. ISSN 1538-3873. DOI: 10.1086/655775. URL http://stacks.iop.org/1538-3873/122/i=894/a=905.

E. Jones, T. Oliphant, P. Peterson, et al. Open source scientific tools for python, 2001.

C. H. Kepner and B. B. Tregoe. Rational Manager. 1965. URL http://agris.fao.org/agris-search/search.do?recordID=US201300461852.

D. M. Kipping and C. Lam. Transit Clairvoyance: Enhancing TESS follow-up using artificial neural networks. Private communication, June 2016.

R. k. Kopparapu, R. Ramirez, J. F. Kasting, V. Eymet, T. D. Robinson, S. Mahadevan, R. C. Terrien, S. Domagal-Goldman, V. Meadows, and R. Deshpande. Habitable Zones Around Main-Sequence Stars: New Estimates. *The Astrophysical Journal*, 765(2):131, Mar. 2013. ISSN 0004-637X, 1538-4357. DOI: 10.1088/0004-637X/765/2/131. arXiv: 1301.6674.

W. B. Landsman. The IDL Astronomy User's Library. volume 77, page 437, 1995. URL `http://adsabs.harvard.edu/abs/1995ASPC...77..437L`.

L. Lyons. *A Practical Guide to Data Analysis for Physical Science Students*. Cambridge University Press, Nov. 1991. ISBN 978-0-521-42463-9. 1996 paperback reprinting.

T. Mazeh, T. Holczer, and S. Faigler. Dearth of short-period Neptunian exoplanets - a desert in period-mass and period-radius planes. *Astronomy & Astrophysics*, 589:A75, May 2016. ISSN 0004-6361, 1432-0746. DOI: 10.1051/0004-6361/201528065. URL `http://arxiv.org/abs/1602.07843`. arXiv: 1602.07843.

W. McKinney. pandas: a foundational python library for data analysis and statistics.

S. M. Mills, D. C. Fabrycky, C. Migaszewski, E. B. Ford, E. Petigura, and H. Isaacson. A resonant chain of four transiting, sub-Neptune planets. *Nature*, 533(7604):509–512, May 2016. ISSN 0028-0836. DOI: 10.1038/nature17445. URL `http://www.nature.com/nature/journal/v533/n7604/full/nature17445.html`.

M. A. C. Perryman, L. Lindegren, J. Kovalevsky, E. Hoeg, U. Bastian, P. L. Bernacca, M. Crézé, F. Donati, M. Grenon, M. Grewing, F. van Leeuwen, H. van der Marel, F. Mignard, C. A. Murray, R. S. Le Poole, H. Schrijver, C. Turon, F. Arenou, M. Froeschlé, and C. S. Petersen. The HIPPARCOS Catalogue. *Astronomy and Astrophysics*, 323, July 1997. ISSN 0004-6361.

E. M. Price and L. A. Rogers. Transit Light Curves with Finite Integration Time: Fisher Information Analysis. *The Astrophysical Journal*, 794(1):92, Sept. 2014. ISSN 1538-4357. DOI: 10.1088/0004-637X/794/1/92. URL `http://arxiv.org/abs/1408.4124`. arXiv: 1408.4124.

G. R. Ricker, J. N. Winn, and R. Vanderspek. Transiting Exoplanet Survey Satellite. *Journal of Astronomical Telescopes, Instruments, and Systems*, 1(1):014003, Oct. 2014. ISSN 2329-4124. DOI: 10.1117/1.JATIS.1.1.014003. URL `http://astronomicaltelescopes.`

spiedigitallibrary.org/article.aspx?doi=10.1117/1.JATIS.1.1.014003.

A. C. Robin, C. Reylé, S. Derrière, and S. Picaud. A synthetic view on structure and evolution of the milky way. *Astronomy & Astrophysics*, 409(2):523–540, 2003.

S. Sharma, J. Bland-Hawthorn, K. V. Johnston, and J. Binney. Galaxia: a code to generate a synthetic survey of the Milky Way. *The Astrophysical Journal*, 730(1):3, Mar. 2011. ISSN 0004-637X, 1538-4357. DOI: 10.1088/0004-637X/730/1/3. URL http://arxiv.org/abs/1101.3561. arXiv: 1101.3561.

P. Sullivan. TESS's Performance on the Kepler Objects of Interest. Technical Report No. 8, MIT, Oct. 2013.

P. W. Sullivan, J. N. Winn, Z. K. Berta-Thompson, D. Charbonneau, D. Deming, C. D. Dressing, D. W. Latham, A. M. Levine, P. R. McCullough, T. Morton, G. R. Ricker, R. Vanderspek, and D. Woods. THE TRANSITING EXOPLANET SURVEY SATELLITE: SIMULATIONS OF PLANET DETECTIONS AND ASTROPHYSICAL FALSE POSITIVES. *ApJ*, 809(1):77, aug 2015. DOI: 10.1088/0004-637x/809/1/77. URL http://dx.doi.org/10.1088/0004-637X/809/1/77.

van Leeuwen and F. v. Leeuwen. Validation of the new Hipparcos reduction. *Astronomy & Astrophysics*, 474(2):12, 2007. DOI: 10.1051/0004-6361:20078357.

S. v. d. Walt, S. C. Colbert, and G. Varoquaux. The NumPy Array: A Structure for Efficient Numerical Computation. *Computing in Science & Engineering*, 13(2):22–30, Mar. 2011. ISSN 1521-9615. DOI: 10.1109/MCSE.2011.37. URL http://scitation.aip.org/content/aip/journal/cise/13/2/10.1109/MCSE.2011.37.

J. Wang and D. A. Fischer. Revealing a Universal Planet–Metallicity Correlation for Planets of Different Sizes Around Solar-type Stars. *The Astronomical Journal*, 149(1):14, 2015. ISSN 1538-3881. DOI: 10.1088/0004-6256/149/1/14. URL http://stacks.iop.org/1538-3881/149/i=1/a=14.

J. N. Winn. Number of Searchable Stars. *TESS Science Memo No. 5, Version 1. Available upon request.*, 2013.